ANALYSIS OF FLOOD FLOWS IN TANA RIVER BASIN USING USGS GEOSPATIAL STREAM FLOW MODEL

A Case Study of Lower Tana River Flood Plain, Kenya

By

Bishar Adan Mohamed

A thesis submitted to the Graduate School in partial fulfillment for the requirements of the Master of Science Degree in Agricultural Engineering (Soil and Water Engineering option) of Egerton University, Egerton, Kenya

January, 2010

DECLARATION AND RECOMMENDATION

DECLARATION

I declare that this thesis is my original work and has not been submitted to any other University for an award of a Degree.

Signed...................................Date...2/02/20.10

Bishar Adan Mohamed

BMII/1321/04

RECOMMENDATION

This thesis has been submitted to the Graduate School for examination with our approval as the University supervisors.

Signed...................................Date...2/02/ 2010.

Prof. J. O. Onyando, Ph.D

Department of Agricultural Engineering

Egerton University,

P.O. Box 536-20115, Egerton, Kenya

Signed...................................Date...2-2-2010

Dr. A. K. Karanja, Ph.D

Department of Agricultural Engineering

Egerton University

P.O. Box 536-20115, Egerton, Kenya

ii

DEDICATION

Thanks to Allah for everything. I dedicate this thesis to my wife Halima M Ismail and our children for their affection, tolerance and moral support.

ACKNOWLEDGMENT

ABSTRACT

Kenya is prone to very serious flood risks especially in lowlands of North Eastern Province (especially Garissa, Mandera and Ijara), Tana River district and areas surrounding Lake Victoria (Nyanza Province). Most of the runoff that causes flooding in lower Tana plain is generated in the upper Tana catchments which receive much higher rainfall than the plains in the downstream reaches. As a result, population living in the plains is often taken unawares. Flood related problems include loss of life, destruction of property , displacement of people, water logging, road network disruption, soil/river bank erosion, mass deposition of sand, health hazards (mosquito breeding) and environmental pollution. As the human and financial costs of disasters rise, there are increasing demands for evidence that mitigation 'pays'. Spatial semi- distributed United State Geological Survey - Stream Flow Model (USGS-SFM) was used in this study for developing non-structural (flood warning system) and structural (identifying flood diversion sites) mitigation measures. USGS-SFM uses globally available terrain, soil and land cover data, and satellite derived estimates of daily rainfall and evapotranspiration. Muskingum-Cunge model was used for river flow routing. During calibration it was found that the correlation of daily simulated and observed stream-flow data of Kazita station (4F19) for the period 1980 to 1982 was 0.8296. The model validation gave a correlation of 0.8064 for Kazita station (4F19) and 0.7389 for Garissa station. The model was found to give short period/lead time of 1 to 3 days forecasting of flood flows between stream's gauging stations. This is enough time to allow for evacuation, and hence reduces the impact of flood damage. Three points were identified as ideal potential sites for inter-basin water transfer by the use of sub-basin physical features generated by the model's complete terrain analysis function and contours from the topo-maps. An estimated magnitude of flood flow (flows above bank-full) at these three un-gauged proposed potential diversion sites have also been determined. Flood warning system through forecasting provides some time for evacuation and other measures. Structural measure (diversion) is an important element for purpose of focusing on the protection of human health and safety, and valuable goods and property. The proposed three inter-basin diversions from Tana to Ewaso Ng'iro Basin will reduce flood damage, open up more land (outside Tana valley) for irrigated food production, improve environment and develop water resources in this arid and semi-arid area.

TABLE OF CONTENTS

CHAPTER 3

LIST OF FIGURES

LIST OF TABLES

LIST OF ABBREVIATIONS

DEM	Digital Elevation Model
EROS	Earth Resources Observation Systems
ESRI	Environmental Systems Research Institute
FAO	Food and Agriculture Organization
FEWS	Famine Early Warning System
GeoSFM	Geospatial Streamflow Model
GIS	Geographical Information Systems
HYRAD	Hydrological Radar
ICRAF	International Centre for Research in Agro-forestry
NEP	North Eastern Province
NOAA	National Oceanic and Atmospheric Administration
OFDA	Office of Foreign Disaster Assistance
PDALE	Provincial Director of Agriculture and Livestock Extension
PPO	Provincial Planning Officer
RCMRD	Regional Centre for Mapping of Resources for Development
UNEP	United Nation Environmental Program
USDA	United State Department of Agriculture
USAID	United State of America International Development
USGS-SFM	United States Geological Survey - Streamflow Model
WMO	World Meteorological Organization

CHAPTER 1

INTRODUCTION

1.1   Background

Floods have profound impact on the quality of life through their destructive losses. These losses are particularly damaging, depriving communities of resources, which could otherwise be used for economic and social development. Flood events are a part of natural hydrological cycle. According to Otieno (2004) floods have existed and will continue to exist. It is becoming evident that, flooding is becoming increasingly a major contributor to personal and to property damage worldwide and in many places it strikes without warning. Although floods are natural phenomena, human activities and human interventions into the processes of nature, such as alterations in the drainage patterns from urbanizations, agricultural practices (irrigation schemes) and deforestation, have considerably changed the situation in whole river basins. Local climatological phenomena, geology, geomorphology, relief, soil, and vegetation conditions also influence flooding. The most extreme floods in several decades (past 44 years) occurred in 1998 in the Asia region, resulting in a total damage estimated over US\$ 23 billion (Omachi and Ti Le-Huu, 2003).

Kenya is prone to very serious flood risks especially in lowlands of North Eastern Province (especially Garissa, Mandera and Ijara) and Tana River district, the areas surrounding Lake Victoria (Nyanza Province) and Nairobi. The El Niño- related floods of 1997/98 necessitated massive relief operation, catching Kenya unprepared, despite warning of strong El Niño event. According to Muthusi (2004) barely a year goes by without reported cases of displacement of people and loss of life and property due to floods in Budalangi (Nzoia River Basin) and Kano plains (River Nyando Basin). In the year 2003, floods damaged crops, livestock, houses, roads, water supply and other infrastructures in North Eastern Province. According to a report by the Provincial Director of Agriculture and Livestock Extension, NEP (2003), the estimated losses associated with floods was over Kshs. 570 Million in Garissa District.

1

The inhabitants of North Eastern Province have learnt "to live with the floods". There is no flood control or flood protection in the study area. This could be due to lack of study on flood protection. The most important economic activity in North Eastern Province is the nomadic pastoralism. However, in a dramatically changing environment and social context (persistent droughts, overgrazing of pastureland/reduction of range resources and creation of many administrative units) some locals are now changing their lifestyle by settling down for irrigated agriculture along Tana River. Irrigation development started in the early 1960s. The potential for Irrigation in North Eastern Province is 42,500 hectares, but only 6,020 hectares has been exploited (PDALE, NEP 2003). Garissa District has a potential of 24,000 hectares (2,500 hectares has been exploited). Hence activities along the riverine flood plain have been on the increase. Tana River as the source of irrigation water has the tendency of changing its course and flooding as a result of the river's bursting its banks. This disrupts agricultural activities from time to time (especially during the rainy season). This is the only agricultural productive area for now. Therefore, flood management is now necessary.

1.2   Statement of the problem

Garissa district riverine flood plain in the Lower Tana basin has been experiencing increase in flooding events. The biannual floods sometimes occur during the short (October–November) and long rainy (April–May) seasons occurring in the catchment area of the upper river basin (Maingi and Marsh, 2001). There is little or no viable economic and social coping mechanisms (preparedness, response and recovery measures) employed by the local community to protect and cope with the effects of the floods. No flood mitigation measures have been put in place and there is no flood warning system to provide time for evacuation and other measures. Flooding has continued to cause destruction of properties (irrigation farms, houses, Livestock etc), displacement, water logging, road network disruption, soil/river bank erosion, mass deposition of sand, health hazards (mosquito breeding) and environmental pollution. The most affected are the poor who inhabit the Lower Tana flood plains trying to eke out a meager living from agriculture and livestock farming.

1.3 Objectives

The broad objective was to evaluate the magnitude of flood flow in Lower Tana to facilitate mitigation and adaptation measures, and economic use of the flood. The following specific objectives were suggested;

1. To simulate flood flow using USGS-Stream Flow Model.
2. To determine potential flood diversion sites and quantify the magnitude of flood flow for economic use.

1.4 Research Questions

1. Can the research be able to evaluate the magnitude of flood flow in Lower Tana to facilitate mitigation and adaption measure, and economic use of the flood?

2. Can the research be able to simulate flood flow using USGS-Stream Flow Model?

3. Can the research also be able to determine potential flood diversion sites and quantify the magnitude flood flow for economic use?

1.5 Justification

Kenya is faced with challenges of increasing population and the need to feed that population and at the same time there are frequent flood water destructions. One possible solution to these problems is to increase water availability through inter-basin transfer. The fundamental concept of this inter-basin water transfer is to collect surplus water during floods from the high precipitation areas of the middle and upper Tana basin and direct it to the adjacent water-deficient areas of Ewaso Ng'iro basin so as to further the economic development mainly through agricultural production and other means.

The rural population of Lower Tana basin essentially depends on agriculture and livestock for livelihood. Extreme demands on natural resources have forced these local people and their livestock to move closer to Tana River basin. The local communities in the Tana flood plain are always at risk of flood disasters. Their vulnerability is high due to combination of physical factors such as exposure to floods, lack of protection infrastructure from flood hazards, and inability to avoid, withstand or recover from the flood hazards.

To improve their welfare implies that land resources must be developed and protected for viable agricultural production. With persistent floods, pre-requisites to sustainable land use for irrigated agriculture in this area have to include effective flood mitigation programme that incorporate non-structural (forecasting floods) and structural (diversion) measures. The approach to flood management in this case comprises the principle of studying the floods and flooding on a basin-wide scale, and, accordingly, further trans-basin (transnational) or inter-basin transfer. The magnitude of adverse impacts of flood depends on the vulnerability of the economic activities, population, the frequency, intensity and extent of flooding (depth and duration of flooding, and the velocities of flows in the flooded areas). According to Duivendijk (1999) extreme flooding may only be influenced to a limited extent and no flood management will ever be able to pre-empt all future flooding, therefore introduction of non-structural measures is vital to decrease damages in case flooding occurs.

The direct benefits of flood management include the reduction in physical damage. Thus, flood damage to crops, cattle, houses, commercial and industrial buildings, and infrastructure etc., will be reduced. Indirect benefits may occur by avoiding disruption to business, transport networks, public services and by avoiding the costs of emergency response and recovery. Below is Table 1.1 showing the potential for Irrigated agriculture of North Eastern Province along Tana and Daua rivers if water is availed through diversion of flood and normal flows. Also some part of dry land farming potential land can also be brought under irrigation by use of the same flood flows.

Table 1.1: Potential for Irrigated and dry land farming, North Eastern, Kenya

District	Irrigation potential (Ha)	Rain-fed potential (Ha)	Total potential (Ha)	Total district area (Ha)
Garissa	24,000	646,000	670,000	3,580,900
Mandera	10,500	25,000	35,500	2,647,000
Ijara	8,000	96,000	104,000	812,200
Total	**42,500**	**828,000**	**884,000**	**12,690,200**

Source: PDALE NEP, 2003

4

CHAPTER 2

LITERATURE REVIEW

Water is the key element in economic, social and cultural developmental of any society. Throughout history, people have settled next to waterways and in flood plains because of the advantages they offer. In spite of these benefits, water can also cause destruction and damage. Floods are among the most devastating natural disasters affecting more people in the world than any other natural disaster. Between 1995 and 2004, floods affected over one billion people and claimed over 40,000 lives (Tokar and Artan, 2005). In addition to humanitarian assistance, USAID/OFDA provides support for programs to mitigate the adverse impacts of floods in Asia and other regions through strengthening flood forecasting and warning capacity of regional and national agencies. An early warning system and preparedness plan are vital tools in reducing loss of life and socioeconomic impacts of floods. A flood early warning system should provide sufficient lead time to prepare for and respond to extreme hydro-meteorological events. The aim is to strengthen the capacity of national hydro-meteorological institutions in climate, weather, and hydrological forecasting to reduce vulnerability and hydro-meteorological hazards of populations at risk. According to a report of UNEP (2002) from 1960 to 1999, floods accounted for about one third of all natural catastrophes in the world, caused more than half of all fatalities, and were responsible for a third of overall economic losses. A study conducted by Manuaela (2004) concludes that major environmental disasters in Africa are recurrent droughts and floods. Their social-economic and ecological impacts are devastating to African countries, because most of them do not have real time forecasting technology of resources for post disaster rehabilitation. Catastrophic floods are numerous in East and Southeast Africa. An example is negative impacts of the 2000 flood in the Limpopo Valley where more than 700 deaths and more than 250,000 displaced people were reported (Famba, 2004). In 2004, floods displaced 24,000 people in Kenya (Abuodha and Omenge, 2004).

Flood-damage mitigation is an embracing method for combating the effects of excess water in streams (Linsley and Franzini, 1979). The accepted structural measures for

5

reducing flood damages are reduction of peak flows by reservoirs, confinement (levees, dykes or a closed conduct), diversion (channel) and river channel improvements (reduction of peak stage by increased velocities). Early Warning System (FEWS) is an effective non- structural measure for flood management. It consists of streamflow monitoring and forecasting.

2.1   Concept of Flooding

Flood is defined as a relatively high flow or stage in a river, markedly higher than the usual (Sharma and Dubey, 2006). If the flows in rivers or streams surpass their carrying capacity, the water spills over to the adjacent lands, causing inundation or flooding. The hydrological cycle, driven by solar energy, provides freshwater resources to the earth through precipitation. Floods are generally an outcome of a complex interaction between natural random processes in the form of precipitation and temperatures with basin/watershed characteristics. Depending on the spatial and temporal distribution and intensities of these precipitations, flood pulses are generated (World Meteorological Organization-No. 1008, 2006). Floods are caused by excessive rainfall or snowmelt or a reduction in a river's conveyance capacity or inadequate design of waterways for cross-drainage works. It's affected by soil moisture level, groundwater level prior to storm, surface infiltration rate (affected by vegetation, soil texture, density, structure and soil moisture), presence of impervious cover, channel cross-sectional shape and roughness and synchronization of run-offs from various parts of watershed. Also it's accelerated by human activities such as land-use practises, occupation of the flood plains, failure of structural flood control measures such as embankments or dams in the upstream and greenhouse gas emissions (which may affect climate change and frequency and magnitude of precipitation events).

Floods can be classified into at least five categories according to the sources of the excess waters. Riverine floods occur when the river run-off volume exceeds local flow capacity due to heavy rainfall in upstream areas, snow melt, tidal influence or failure of flood control works upstream (World Meteorological Organization, 2006). Flash floods (more destructive than other types of flooding) occur as a result of the rapid accumulation and release of runoff waters from upstream mountainous areas, which can

6

be caused by heavy rainfall, cloud bursts, landslides, the sudden break-up of an ice jam or failure of flood control works. Coastal floods (Tsunamis) are mainly triggered by powerful offshore earthquakes, volcanic eruptions, high tides and storm surges. Local floods/Urban floods are caused by very high rainfall intensity, long duration or seasonal storms (World Meteorological Organization, 2006). This type of flood normally occurs as a result of flood flow exceeding the local drainage capacity.

Floods provide variable river flows and are an intermittent source of freshwater supply, important source for restocking local man-made water sources such as ponds, reservoirs, dams and recharging groundwater (World Meteorological Organization-No. 1008, 2006). Flood waters carry nutrients and sediments, which are deposited on flood plains. These deposits enrich the soil fertility. River basin is an ecological unit interconnecting upstream spawning habitats with downstream rearing habitats for a variety of fish species and other aquatic systems. It provides an ecological trigger for both the spawning and migration of certain species. Flood helps in rejuvenation of the river ecosystem (fish, wildlife and waterfowl). Seasonal variability and variable sediment and flow regimes help maintain ecological biodiversity in rivers and flood plains.

Major and immediate impacts of flooding include loss of physical life, damage to property, destruction of crops, loss of livestock, non-functioning of infrastructure facilities and deterioration of health condition owing to waterborne diseases. Flood cause loss of livelihoods: As communication links and infrastructure (clean water and electricity, transport, communication, education and health care) are damaged and disrupted, economic activities come to a standstill, resulting in dislocation and the dysfunction of normal life for a period much beyond the duration of the flooding (World Meteorological Organization-No. 1008, 2006). (World Meteorological Organization-No. 1008, 2006). Agricultural productions are put out of work for long periods owing to the loss of crop seasons. The spillover effects of the loss of livelihoods can be felt in business and commercial activities in adjacent non-flooded areas as well. Frequent flooding, resulting in loss of livelihoods, production and other prolonged economic impacts and types of suffering can trigger mass migration or population displacement.

2.2   Methods of flood flow determination

The flood parameters whose values can represent the magnitude or phenomenon of a flood and the damage caused by it at a certain location are maximum discharge during flood, maximum water level, maximum extent of flooding, duration, bank overspill in a certain area and duration of the actual flood wave travelling down the river. Flood frequency curves (exceedance curves) are drawn up for values of the selected flood parameter. According to Duivendijk (1999) these exceedance curves establish the relationship between various flood parameters, that is total discharge over and above a certain flood level verses the bank overspill; maximum discharge during a flood verses the duration of flooding; maximum discharge during a flood verses the bank overspill and maximum water level during a flood verses the extent of flooding.

2.2.1   Flood Flow Measurement

Flood can be measured directly by using periodic meter of daily flows at gauging stations. Here the height on the meter is converted into discharge by use of rating curves. According to Linsley et al (1992) the relationship of the stage and discharge is given by;

$$Q = K (H - b)^n \tag{2.1}$$

where Q is discharge (meter^3/second), H is height or water surface elevation (meter), b is the stage of zero flow (meter) and K and n calibration variables determined through the logarithmic regression procedure. For each transection, the height or stage of zero flow is determined through an iterative process with the goal of maximizing the correlation (as measured by r^2) between stage and discharge. This is the method used in determining daily flows at the gauged stations along Tana River by Ministry of Water and Irrigation and Dwars Heederik en Vertey (DHV) during their study on Lower Tana River morphology (1986).

Flood can also be expressed by applying continuity equation (Chow et al, 1988) as;

$$Q = 1 / n * A * R^{2/3} * S^{1/2} \tag{2.2}$$

where n is manning's roughness coefficient, A is cross-sectional area and R is hydraulic radius and S channel slope. Cross-sectional area is determined by leveling (dividing the river cross-section into many sections and taking details of each). The slope is determined

8

by using the river section with a good stretch carrying sufficient water level that can used in determining the water surface slope at the time of pick flow. Tracer (injects impulses at interval between two points), moving boat, ultra sound or magnetic methods can be used in determining the pick flood flow's velocities and discharges. This method can be used for determination of bank-full flows at any section of the Tana River. This bank-full can be compared with the one determined by USGS Stream Flow model.

2.2.2 Geographic Information Systems (GIS) Application

GIS is the process of digitally storing and producing useful maps from geographic data. The management and planning of natural resources such as water resources have often been done, particularly in developed countries, using GIS and remote sensing technology (Onyando *et al*, 2005). According to Hudgens and Maidment (1999) relationship between GIS and hydrological models has evolved over time. The first method, hydrological parameter determination, simply uses GIS to read parameters from existing data sets. This is a straightforward application of a GIS system to extract spatial data. In the second method, hydrological parameters are developed from basic data sets. In other words, basic spatial data sets are processed within the GIS according to programmed assumptions and algorithms. The advantage of using GIS in hydrologic modeling is to provide spatially derived hydrologic parameters (such as watershed area, curve number, precipitation, flow length in each watershed, and slope) for input into hydrologic models such as Geospatial USGS Streamflow Model (Anderson, 2000). This model has water balance, catchment routing, and distributed channel routing sub-modules in flood simulation and determination at catchment scale.

GIS is a large database management system that contains both spatial and non-spatial data for policy and management decision-making. These data can include values of ground surface elevation, land coverage, population densities, and just about any type of information that varies spatially (Snead, 2000). A vector structure stores data or features as points, lines, or polygons that are defined by a set of Cartesian coordinates. Each feature in a vector layer can have many attributes associated, a raster structure stores data as a regular array of cells, such as in satellite image data, or in generalized data that could be obtained by laying a grid over the landscape. The integration of

9

hydrology and GIS involves spatial data construction, integration of spatial model layers and GIS-model interface. It can assist in design, calibration and modifications of models.

2.2.3   Flood Forecasting

With longer or shorter lead times, depending on the drainage basins and hydro-meteorological parameters, flood forecasting can permit the prediction of the progress of floods, enabling the responsible authorities and involved populations to take personal, material and organizational decisions to reduce the detrimental consequences of the imminent flood (Duivendijk, 1999).

Flood-forecasting techniques include forecasts of meteorological parameters (rainfall, intensity, timing and duration), hydrological process model (meteorological and hydrological inputs, depth and discharge, downstream flow as output) and mathematical hydraulic models (description of river channel and characteristics of the flood). The basis of flood forecasting is the analysis and interpretation of all available data from preceding or initiating events (input variables) which create or contribute to the development of flooding at some other, downstream point of the drainage basin in a future time (output variable) whatever the future uncertain events (Duivendijk, 1999). The period which separates the acquisition of data and the reality of the forecasted event can vary from one hour or less for small basins to several days for basins of hundreds or thousands of square kilometers.

USGS Geospatial Stream Model uses above input variables in flood forecasting for three days. Flood peak events are put into the river channel geometry in order to forecast flood level at different points along the river. It computes flow statistics (max, min, mean, 25, 75, 33, 66 and 50 percentile flow). It ranks and display current flows relative to percentile flows (high, low, medium). The model also performs inundation mapping (based on uniform flow depths within each river reach) and display hydrographs where needed.

2.3   Flood Modeling

Hydrological models are tools that are essential for hydrological data analysis needed in solving problems related to flooding in hydrology. They can be classified as

empirical, conceptual or combination of both. Empirical models are used for converting rainfall volume into runoff volume. It does not take account of hydrologic concepts (only uses mathematical equations without relation to the system's physics). Conceptual models use the hydrologic concepts in order to simulate the basin behavior. Conceptual models usually have two main components: (a) rainfall – runoff module that transforms rainfall into runoff through analysing various hydrologic components such as interception, upper soil zone, groundwater and overland flow; (b) routing module, which simulates the flow in the rivers and reservoirs. Rainfall – runoff models can be lumped or distributed. Lumped models do not usually take into account the spatial variability of rainfall, state variables and model parameters. The advantage of distributed models is that they can take into account the spatial variation of physical characteristics of the basin and rainfall conditions (Wheater, 2004).

Rainfall – Runoff Modeling can be used to predict flood hydrographs for sub-catchments and whole catchment. The modeling approach in general depends on the required scale of the problem (space-scale and time-scale), the type of catchment, and the modeling task. Typical tasks for these simulation models include modeling existing catchments for which input-output data exist, runoff estimation on ungauged basins, prediction of effects of catchment change (land use change), coupled hydrology and geochemistry (Nutrients, Acid rain), coupled hydrology and meteorology (Wheater, 2004). This rainfall-runoff model assumes only about flood wave spread and does not take into account attenuation of flood waves (Muthusi, 2004).

Flood routing is the procedure to predict the outflow hydrograph at a point downstream in a river (or reservoir) as a function of the inflow hydrograph at a point upstream. As flood waves travel downstream their variable speed, attenuation and flood storages are considered. Routing techniques can either be hydraulic or hydrologic in nature (Choudhury *et al*, 2002). Hydraulic routing techniques are based on the solution of the partial differential equations such as St. Venant or the dynamic wave equations of unsteady open channel flow. It is only within the last four decades that the mathematical complex St. Venant equation could be solved via computers with varying degrees of feasibility (Fread, 1993). Hydrologic routing employs the continuity equation and an analytical or an empirical relationship between storage within the reach and discharge at

the outlet. In this study distributed Muskingum-Cunge hydrologic routing method has been used. Advantage of hydrologic routing over hydraulic routing techniques are that solution is obtained through a linear algebraic equation instead of a finite difference to characteristic approximation of a partial differential equation; this allows the entire hydrograph to be obtained at required cross section instead of requiring solution over the entire length of the channel for each time step, as in kinematic wave method. It also shows less wave attenuation, permitting a more flexible choice to time and space increments for the computation as compared to the kinematic wave method. Disadvantages of Muskingum-Cunge method in the USGS Stream Flow Model is that it cannot handle downstream disturbances that propagate upstream.

2.4   Flood Models

Mozambique is highly vulnerable to weather-related natural disaster with both drought and floods affecting the country, especially the Limpopo basin. The Over Land and Channel Flow module of SOBEK two-dimensional model was used to define areas at hazard and generate flood map for the study area. To produce these maps, GIS, RS and the flood modeling were used. The model results consisted of a set of maps showing flood starting time, flow velocity, and water depth for mild, moderate and severe flood type (Shaviraachin, 2005).

Flood hazard assessment on Lower Bicol floodplain, Philippines was done using 2D flood model Delft-FLS. The Model parameters were the DEM of the floodplain, the DEM of the riverbed, the floodplain and riverbed roughness, and the artificial structures. It was finally concluded that the 2D modeling approach is useful for reconstruction of past flood events. The model results suggested that the flood parameters (water depth and flow velocity) were not very sensitive to variations in surface roughness. However physical barriers, like embankments affect flooding significantly (Otieno, 2004).

USGS-SFM Model has high performance potential. It was also applied to the 3,587 km^2 Nyando River basin in western Kenya with the aim of evaluating its performance as a tool for flood early warning (Muthusi, 2004). From this study, the high correlation coefficients (R^2 values of 0.72 and 0.83) between simulated and observed streamflow for the model calibration and validation respectively at the most downstream

gauging station implied sufficient performance of the model in streamflow generation (Muthusi, 2004). Also according to Muthusi (2004) where ground based rainfall data is not sufficient for use in the model, satellite rainfall data can be used as an alternative. Model validation in the Nzoia and Limpopo river basins were satisfactory (Artan *et al*, 2001). USGS-SFM hydrologic model was used in this study. This model was selected because it could develop both non-structural (flood warning system) and structural (identifying flood diversion sites) mitigation measures. The flood forecasting part of the model would mitigate flood damage by providing adequate technical advice to the communities in order to prepare in advance of the floods, and the structural mitigation measures would be used for determining the diversion off-take sites and their flood magnitude.

2.5   Integrated Flood Management

Increase of population in flood prone areas together with a higher standard of living, destruction of ecological values, intensive land use and the knowledge that extreme floods will cause flooding (and is unavoidable) will require wide range of flood management measures. According to Yap (2009) flood management practices largely focuses on reducing flooding and susceptibility to flood damage through structural and non-structural interventions. The structural methods used in flood management are storage of flood waters (part of) in upstream reservoirs and increase in discharge capacity of the river system (e.g. diversion or bypass channels, channel deepening or widening). Non-structural approaches in flood management fall naturally into planning and response measures (World Meteorological Organization, 2004). Planning stage has anticipatory measures which can be assessed, defined, and implemented in the flood plains to reduce the risk to property from identifiable potential floods. This includes flood forecasting, control of flood plain development, flood insurance, flood proofing and catchment management. Planning emergency response measures which are applied when a damaging flood is forecast, imminent or underway, to help mitigate its damaging effects. This includes flood emergency response planning, flood fighting, flood warning, evacuation, emergency assistance and relief. Flood management involves the protection of people and their socio-economic activities in flood plains from flooding (Integrated

Water Resources Management-WMO No.1010). Flood control and protection have been engineering-centered, with little or no consideration being given to the social, cultural and environmental effects of the selected strategy, nor to long-term economic concerns. Flood management strategies that largely rely on structural solutions alter the natural environment of the river course. This results in loss of habitats, biological diversity and ecosystem productivity. For sustainable development in the flood plain it's important to address the negative consequences of flood control and protection measures on the environment. This has led to a paradigm shift from flood control to flood management (Integrated Water Resources Management-WMO No.1010). Environmental degradation has the potential to threaten human life and livelihoods, food and health security. It will also destroy the natural ecosystems, which are highly resilient, at the same time difficult to restore. Therefore, integrated flood management includes the improvement of the capacity of ecosystems to absorb continuous disturbances, so that they continue to provide the required services. It is, therefore, extremely important to balance development imperatives, flood risks, social and economic vulnerability, and sustainable development vis-à-vis the preservation of ecosystems (World Meteorological Organization No-1009, 2006). Integrated Flood Management involves flood control and protection through structural and incorporation of complementary non-structural measures (flood forecasting and land use regulations). It maximizes the net benefits from flood plains and minimizes loss of life from flooding through adoption of basin and multidisciplinary approach, reducing vulnerability and risks due to flooding, enabling community involvement and preserving ecosystems.

According to Deputy Prime Minister and Minister for Finance (2009) the Japanese Government has given a grant of approximately Kshs.422.3 million to Kenya Government for Community Based Flood Disaster Management Project to adapt to Climate change in the Nyando River Basin. The flood management systems which will be implemented are structural and non -structural measures for integrated flood management in 24 villages of flood prone areas of Nyando and Kisumu Districts. Some of the structural measures to be undertaken include; construction of boreholes, evacuation centres and storage facilities. The development of community based flood management organizations, community flood management training and education program for disaster

14

prevention will be undertaken under the non-structural measures. Adaptation of floods includes avoiding the floods through early warning, living with floods by incorporation integrated solutions for adaptation of life/property and controlling the flood through infrastructure works and proper land use.

2.6 USGS Stream Flow Model

USGS Stream Flow Model is a spatially distributed, physically based hydrologic model. Data needed by the model includes daily precipitation and evaporation, topography, hydrologic network, land use and soils (Artan *et al*, 2001). It consists of a GIS-based module, used for model input and data preparation, and the rainfall-runoff simulation model. The rainfall-runoff model is comprised of a soil and water accounting module that produces surface and sub-surface runoff for each sub-basin, an upland headwater basins routing module, and a major river routing module. The runoff-producing mechanisms are surface runoff due to precipitation excess, rapid subsurface flow (interflow), and base flow. The surface upland routing is a physically based unit hydrograph method that relies on cell-based landscape attributes such as drainage area, slope, flow direction, and flow length derived from a digital elevation model. The interflow and base flow components of the runoff are routed with a set of theoretical linear reservoirs. In the main river reaches, water is routed using a nonlinear formulation of the Muskingum-Cunge routing scheme. To simulate daily streamflow, information is needed to define the aerial extent of the watershed being modeled, physical characteristics, precipitation falling, and moisture losses due to evapotranspiration.

2.6.1 Satellite Rainfall Estimates (RFE)

National Oceanic and Atmospheric Administration (NOAA)'s Climate Prediction Center produces daily grid rainfall estimates (RFE) for Africa since 1995. These Satellite rainfall estimates are used for geospatial stream flow modeling. USGS-SFM model uses methods for spatial integration of the RFE over topologically linked river basins derived from a 1-km digital elevation model. These accumulations are compared with long-term average values to derive a flood risk score.

2.6.2 Precipitation

Daily meteorological station rainfall is required to generate rainfall grids for the entire sub-basin through interpolation method. These grids will generate rain text file as an input for flow routing. Excess rainfall occurs when rainfall rate is higher than infiltration rate. Soil Conservation Service (SCS) curve number is used in determining excess rainfall (Artan *et al*, 2001).

2.6.3 Soil Data

Soil data can be acquired from Kenya Soil Survey. It can also be downloaded from FAO digital soil map of the world (http://www.fao.org/ag/agl/agll/prtsoil.htm). The soil data describes the average water holding capacity of the soils (millimeters), average hydrologic active soil depth (centimeters), textual description of the, average saturation soil hydraulic conductivity (meters per hour), average Soil Conservation Service (SCS) curve number for the soils, maximum percentage of the watershed which can be impervious, and minimum percentage which can be impervious for each sub-watershed that makes up the watershed being modeled (Artan *et al*, 2001).

2.6.4 Terrain Analysis

According to Hudgens and Maidment (1999) DEM is used as the basic spatial data source in defining the hydrography of the study basin. The analysis of topographic data for hydrologic modeling applications relies on the simple principle that water flows in the direction of steepest descent (Asante *et al*, 2008). Arc View's terrain analysis function determines flow direction, flow accumulation, flow length, hill length, slope, sub-basins and downstream sub-basin. Basin boundaries and stream networks were also delineated. Terrain analysis function divides the study area into smaller sub-basin and rivers, establish the connectivity between these elements and computes topography dependent parameters of the model (Artan *et al*, 2001). The following grid themes are created:

1. *Flow direction–grid theme* "FlowDir" is created using spatial analyst function "Flow Direction" and the corrected DEM grid theme. Each cell in the flow direction grid is assigned an integer value based upon that cell's corresponding cell value in the processed DEM grid theme relative to the values of the

surrounding cells in the processed DEM grid theme.
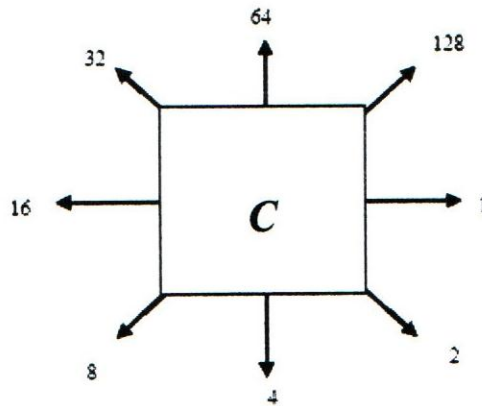
As example for cell "*C*", if the cell, corresponding to the upper right cell, contains a corrected DEM value less than the corrected DEM values for all other surrounding cells, the flow direction grid theme for cell "*C* is assigned a value of 128.

2. *Flow accumulation–grid theme* "FlowAcc" identifies the number of cells flowing into a particular cell by using the function "FlowAccumulation" and the flow-direction grid theme.

3. *Flow length–theme* "FlowLen" is the distance water would travel to reach this cell by using the function "FlowLength" and the flow-direction grid theme.

4. *Streams–grid theme* "Streams" is created using the flow-accumulation grid theme and a threshold value. The threshold value is the number of cells that must be flowing into a cell before that cell is identified as being part of a stream network.

5. *Stream Links–grid theme* "StrLinks" is created using the function "StreamLink" and the flow-direction grid theme. This function results in a grid theme that assigns a unique value to sections of a stream between points of intersection.

6. *Outlets–grid theme* "Outlets" is created using stream-links and flow accumulation grid themes to identify the cells representing the most downstream point on a stream link, the watershed outlet.

7. *Basins–grid theme* "Basins" shows the drainage area above each of the watershed outlets identified in the outlet grid theme and is created using the function

17

"Watershed", the flow-direction and the outlet grid themes.

8. *Hill slope length–grid theme* "HillLength" is created using the function "FlowLength", flow-direction and stream grid themes. A temporary flow-direction grid is created where the flow direction of all cells identified as a stream in the streams grid theme are set to a no-value indicator.

9. *Terrain slope–grid theme* "Slope" is created using the function "Slope" and the corrected DEM grid theme. Its calculated using the formula,

   a. *rise_run = SQRT(SQRT(dz/dx)+SQRT(dz/dy)*

   b. In the following 3x3 grid, dz/dx and dz/dy for cell "e" was computed as;

a	b	c
d	e	f
g	h	i

   i. *(dz/dx) = ((a + 2d + g) - (c + 2f + i)) / (8 * x_mesh_spacing)*

   ii. *(dz/dy) = ((a + 2b + c) - (g + 2h + i)) / (8 * y_mesh_spacing)*

   c. where *x_mesh_spacing* = horizontal distance of the grid
      y_mesh_spacing = vertical distance of the grid

10. *Downstream ordering–grid theme* "Downstream" in is created using the neighborhood function, the outlet and basins grid themes. This function creates a grid theme where the value for a watershed is greater than the values for watersheds upstream of that watershed.

2.6.5 Water Balance

The goal of Water Balance is in the model is to separate input rainfall into evapotranspiration, surface, interflow, base-flow and ground water components at the end of each simulation time step (Artan *et al*, 2001). The concept of water balance is illustrated in Figure 2.1. Each soil layer includes water bound by tension (adhesion and

cohesion) and free water (moving under gravity). Free water can be lost by evapotranspiration, percolation and transpiration in the active upper zone. Also in the lower soil layer zones free water loss is transpiration and percolation. According to Artan *et al* (2001) soil water content (*SW*) is determined by;

$$SW = PR - ET - SR - SSR - G_W \qquad (2.3)$$

where *PR* is precipitation, *ET* is Evapo-transpiration, G_W is groundwater loss by deep percolation. *SR* is surface runoff and *SSR* is sub-surface component.
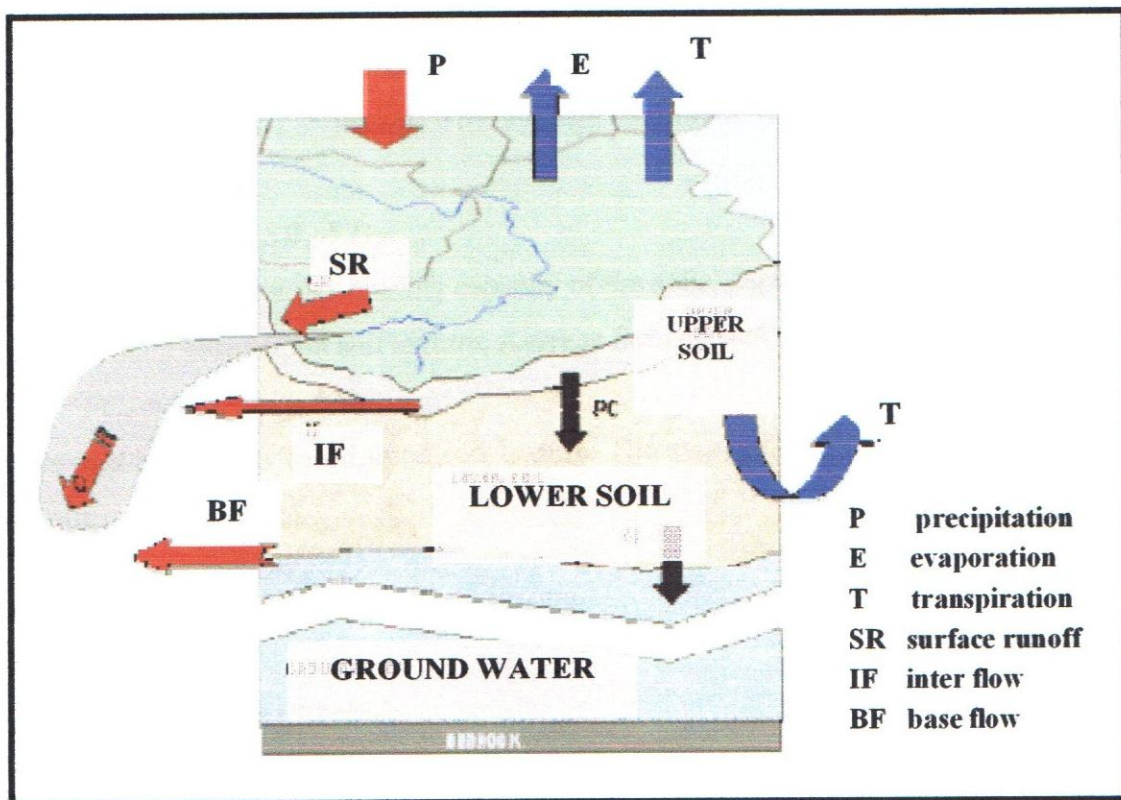
Figure 2.1: Conception of the Stream Flow Model (SFM) (Source, USGS, 2001)

2.6.6   Unit Hydrograph

The Unit Hydrograph (UH) of a watershed is defined as the direct runoff hydrograph resulting from a unit volume of excess rainfall of constant intensity and uniformly distributed over the drainage area. It's the processes of transformation of rainfall into a flood hydrograph and the translation of that hydrograph throughout a watershed. In the USGS-SFM model, GIS is used to describe the connectivity of the links

19

in the watershed-flow network, making the unit hydrograph spatially distributed. The GIS based approach permits the spatial pattern of excess rainfall over the whole catchment (Muthusi, 2004). Direct surface runoff (SR) at the watershed outlet is given by;

$$SR = PE * A / \Delta t \tag{2.4}$$

where PE is excess rainfall, A is area and Δt is rainfall duration.

2.6.7 Antecedent Soil Moisture

According to Artan *et al*, (2001) soil layer is divided into two layers, a top (10%) and a deeper layer (90%). The initial water content (WC_{iu}) in the top (0.05 * FC_a) and deeper (0.75 * FC_a) root zones is a function of the average field capacity (FC_a). The depth of water in meters, in the main channel is a function of the channel's width (*Average depth = 0.01 * width*). The average minimum soil-water content (SW_{am}) is computed as;

$$SW_{am} = min * SW_a * D_{sl} \tag{2.5}$$

where SW_a is average water holding capacity of the soils, D_{sl} is depth of the soil layer and *min* is constant based upon soil texture. Average field capacity (FC_a) is computed as;

$$FC_a = mid * SW_a * D_{sl} \tag{2.6}$$

where *mid* is constant based upon soil texture. The average saturation capacity (SC_a) of the soils is computed as;

$$SC_a = max * SW_a * D_{sl} \tag{2.7}$$

where *max* is constant based upon soil texture.

2.6.8 Flow Routing Module

Surface runoff can be classified into overland flow and channel flow. Flow routing at sub-basin level is done by using a set of conceptual linear reservoirs for sub-surface (inter-flow and base-flow). Kinematic wave equation combined with Manning is modified for use within GIS setup in determination of surface runoff (Artan *et al*, 2001). It relies on cell-based landscape attributes such as drainage area, slope, flow direction, and flow length derived from a digital elevation model. Muskingum-Cunge model is used for flow routing in the river channel network (Chow *et al*, 1988).

According to Artan *et al* (2001) excess precipitation and water in the stream

channel is routed downstream using lag coefficients. Excess water (SW_e) is given by;

$$SW_e = SW_{uz} - (FC * \% D_{us})$$

(2.8)

where D_{uz} is soil depth in the upper soil zone. SW_{uz} is Soil Water content of upper soil layer and FC is field capacity. The GreenAmpt model will compute the portion of the excess soil water available for interflow and base flow. Brooks Corey is used to compute the wetting suction of the lower soil zone.

2.6.9 Digital Elevation Model

USGS-SFM model uses ESRI's ArcView GIS and the ArcView extension "Spatial Analyst." Grid of elevation data for describing the physical characteristics of each sub-watershed are created using digital elevation model (DEM) data available from U.S.G.S's http://edcdaac.usgs.gov/gtopo30/hydro/africa.html Web-site. This data set is an image of corrected -DEM data on a one-square kilometer grid for all of Africa. The watershed is divided into grid cells of an available digital elevation model (DEM).

2.7 Muskingum-Cunge Routing Method

Muskingum-Cunge channel routing technique is a nonlinear coefficient method that accounts for hydrograph diffusion based on physical channel properties and the inflowing hydrograph (US Army Corps of Engineers, 1998). The basic formulation of the equations is derived from the continuity equation with lateral inflow (q_L)

$$\frac{\partial A}{\partial t} + \frac{\partial Q}{\partial x} = q_L$$

(2.9)

and the diffusion form of the momentum equation:

$$S_f = S_o - \frac{\partial Y}{\partial x}$$

(2.10)

By combining equations (2.17) and (2.18) and linearizing, the following equation is formulated (Miller and Cunge, 1975):

$$\frac{\partial Q}{\partial t} + c\frac{\partial Q}{\partial x} = \mu \frac{\partial^2 Q}{\partial x^2} + C q_L$$

(2.11)

where Q is discharge, A is flow area, t is time, x is distance along the channel, Y is depth of flow, q_L is lateral inflow per unit of channel length, S_f is friction slope, S_o is bed slope

21

and C is the wave celerity in the x direction. The wave celerity (C) and the hydraulic diffusivity (μ) are expressed as follows:

$$C = \frac{dQ}{dA}$$

$$\mu = \frac{Q}{2BS_o} \tag{2.12}$$

where B is the top width of the water surface. The convective diffusion equation (2.11) is the basis for the Muskingum-Cunge method. In the original Muskingum formulation, with lateral inflow, the continuity equation (2.9) is discretized on the x-t plane (Figure-2.2) to yield:

$$Q_{j+1}^{t+1} = C_0 Q_j^t + C_1 Q_j^{t+1} + C_2 Q_{j+1}^t + C_3 Q_L \tag{2.13}$$
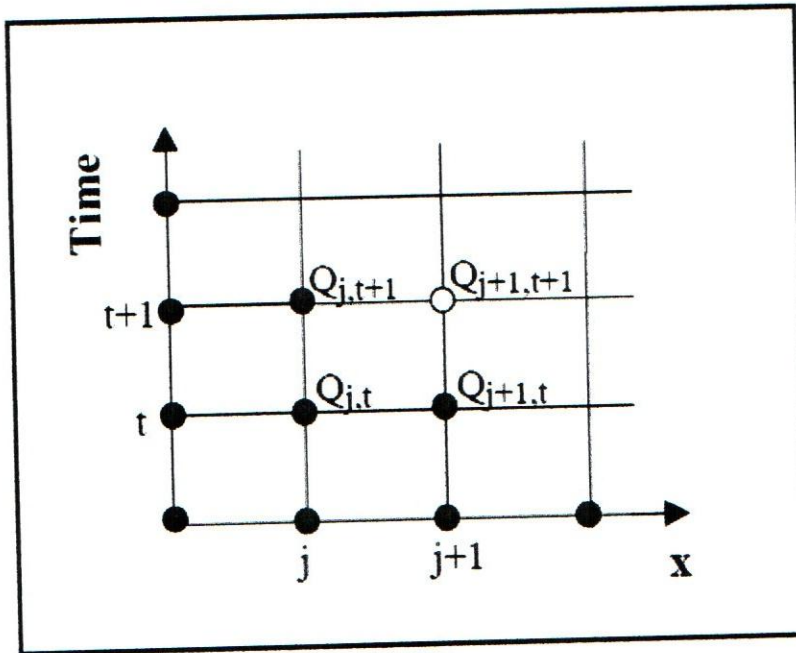
Figure 2.2: Discretization of the continuity equation on x-t plane

It is assumed that the storage in the reach is expressed as classical Muskingum storage:

$$S = K [XI + (1 - X) O] \tag{2.14}$$

where S is channel storage, K is cell travel time (seconds), X is weighting factor, I is

22

inflow and O is outflow. Therefore, the coefficients can be expressed as follows:

$$C_0 = \frac{\frac{\Delta t}{K} + 2X}{\frac{\Delta t}{K} + 2(1-X)} \tag{2.15}$$

$$C_1 = \frac{\frac{\Delta t}{K} - 2X}{\frac{\Delta t}{K} + 2(1-X)} \tag{2.16}$$

$$C_2 = \frac{2(1-X) - \frac{\Delta t}{K}}{\frac{\Delta t}{K} + 2(1-X)} \tag{2.17}$$

$$Q_L = q_L \Delta X$$

$$C_3 = \frac{2(\frac{\Delta t}{K})}{\frac{\Delta t}{K} + 2(1-X)} \tag{2.18}$$

For a calibrated set of K and X values the computed routing coefficients add up to unity ($C_0 + C_1 + C_2 = 1$). The value of X varies between 0.0 and 0.5. Cunge evaluated the diffusion that is produced in the Muskingum equation and analytically solved for the following diffusion coefficient:

$$\mu_o = C \Delta X [\frac{1}{2} - X] \tag{2.19}$$

In the Muskingum-Cunge formulation, the amount of diffusion is controlled by setting equation (2.11) and (2.14) equal to each other. The Muskingum-Cunge equation is therefore considered an approximation of the convective diffusion equation (2.10). As a result, the parameters K and X are expressed as follows (Chow et al, 1969).

$$K = \Delta X / C \tag{2.20}$$

$$X = \frac{1}{2} [1 - Q / B S_a C \Delta X] \tag{2.21}$$

where Q is discharge, B is width of water surface, S_a is channel bed slope and C is the wave celerity corresponding to discharge (Q). The model starts channel routing with the most upstream watershed and estimates the initial stream-flow as being the stream-flow needed to achieve a bank full condition. This bank full stream-flow condition is a

function of total area above the watershed outflow. The bank-full discharg[e]
channel cross-sections can also be obtained from Manning's equation (Cho[w]
The model also estimates the depth of the stream-flow (D_f) based on cha[n]
slope, width and manning's coefficient. The model executes a loop t[o]
Muskingum weighting coefficient (X), proportionality coefficient (K), space step (ΔX)
and time step (Δt).

2.8   Methods of Estimating Missing Data

This involves estimating missing data on rainfall, evaporation and streamflow. A proportion method will involve the calculation of the annual arithmetic mean values from nearby station gauges and using them to fill up the gaps of the corresponding years without data. It's based on the assumption that, gauges that were spatially close to each other tend to show similar flow characteristics. Calculation of missing data can also be based on correlation and linear regression analysis for best-fit stations.

2.9   Calibration and Validation

The calibration procedure aims at estimating parameter values that cannot be accessed directly from field data. The goal of calibration and testing is to reduce the overall uncertainty of simulation. During the calibration process, different accuracy criteria is used to compare the simulated and measured data. According to Nash and Sutcliffe (1970) performance criteria (E) for relating observed and simulated output of the model was determined by;

$$E = [\sum (O - O_a)^2 - \sum (O - P)^2] / \sum (O - O_a)^2 \qquad (2.22)$$

where O is the observed runoff volume, O_a the observed average, and P is the estimated runoff volume. E values over 0 indicate the efficiency of the model is better than the average of observed runoff volume. A value of 1 indicates a perfect model fit. A negative value of E indicates the model is performing more poorly than simply using the average of the observed data. According to McCuen *et al* (2006) Nash–Sutcliffe performance criteria is a widely used and potentially reliable statistic for assessing the goodness of fit of hydrologic models. In the case of gauged catchments, Nash cascade model parameters can be determined through the method of moments or calibration using observed runoff

hydrograph (Patil, 2008). However, for ungauged catchments the parameters must be derived indirectly through a regionalization procedure. Onyando (2005) applied transfer functions for Nash cascade model parameters by use of the conventional two step regionalization procedure, in which model parameters were first calibrated separately for each catchment in a set of gauged catchments, then the transfer functions for the parameters were derived through regression procedures.

The USGS SFM model is normally calibrated and validated by the use of monthly and annual flow statistics series. Correlation coefficient(r) is used for assessment of model's performance by comparing the predicted and observed data. Correlation coefficient(r) is given by;

$$r = 1 - S^2 / (\sigma_y)^2 \quad \text{and} \quad S = \{\sum(y_f - y_o)^2 / (n-1)\}^{1/2} \qquad (2.23)$$

Where r is coefficient of determination ($|r| = 1$), S is standard error, σy is standard deviation, yf is measured value and yo is mean value.

2.10 Model Simulation

Model simulation is an iteration process which starts by advancing a candidate model which from graphical inspection of data appears likely to represent their expected characteristics. These values are plotted and compared with observed data in determination of candidate model's failure. According to Muthusi (2004) the discrepancies between the fitted and observed value gives clues as to how the candidate model should be modified. This is repeated until the two agree within acceptable range.

2.11 Inter-Basin Water Transfer

According to Biswas (1983) water is a resource and there is no danger that the world is going to run out of water due to hydrological circle effects. However, the main problem with water is that its distribution varies tremendously both with respect to time and space, and accordingly its rational management is low due to poor efficiency in its uses. Water is mainly used for domestic, irrigation, hydroelectric power generation, navigation, recreation and fisheries development. On a global basis, agriculture is the largest user of water and accounts for nearly 80 per cent of total consumption (Biswas, 1983). According to Ministry of Water & Irrigation (2006), water withdrawal in Kenya

for agricultural, domestic and industrial purposes was 2.05 km³ in 1990, of which 1.6 km³ was for agriculture. There is low level development of water resources in Kenya, estimated at less than 20% (1.6 billion cubic meters per annum) against the surface water potential of 7.4 billion cubic meters and groundwater potential of 1.0 billion cubic meters per annum. The country is water scarce category of 647 m³ per capita against the global benchmark of 1000 m³ (Ministry of Water & Irrigation, 2006).

According to Northern Service Water Board (2006) the technicality on the inter-basin water transfer from Tana to Ewaso Ng'iro north basin was acceptable to main stakeholders of Tana river basin. These stakeholders were all Water Service Boards, Tana and Athi Development Authority, National Irrigation Board, Water Resources Management Authority, Kengen, Water Cooperation and Pipeline and Kenya Wildlife Service. Also according to Water Resources Management Authority (Kenya), one of their strategies on flood mitigation is the development of flood control infrastructure (Ministry of Water & Irrigation, 2006). The Yatta Canal (60 Kilometers long) involves an inter-basin transfer of water from Tana to Athi River catchment. It supplies water for domestic, livestock and irrigation in Machakos and Kitui areas. The construction of Yatta Canal started in 1953 and was commissioned in 1958 (Wambua, S., 2003). Nairobi lies in the upper part of the Athi Basin. The bulk of its water supply is through inter basin transfer from the Tana to Athi Basin (United Nation-World Water Development Report, 2006).

2.12   Previous Studies on Tana River

According to Agwata (2006) Tana is the longest river in Kenya, it covering a distance of about 1,012 kilometers from the farthest source to the Indian Ocean. It has an annual mean discharge of five billion cubic meters of water. It is situated between latitude 0^0 30' north and 2^0 30'south and longitude of 37^0 00' and 41^0 00'. The main tributaries are Gura, Ragati, Chania, Thiba, Kazita, Ura, Mitonga, Sabasaba, Mathioya and Ena. Tributaries emanate from Mount Kenya and Nyambene Hills. The whole catchment area of the Tana River is about 100,000 km², covering about 20% of the land area of the country. It has three major water towers namely Mt. Kenya in the North and North East contributing about 49% of runoff, the Aberdare Ranges to the West contributing about 42% and the Nyambene Hills to the East of the basin contributing

26

nearly 7% of the total runoff in the basin (Water Resources Management Authority, 2006). This catchment holds a major portion of Kenya's agricultural potential (530,000 ha) and is the main source (80 %) of hydro-electric power (Ministry of Water & Irrigation, 2006). It sustains a population of about five million people (Agwata, 2006). The seven folk hydro-electric generating dams store large quantities of water in several man-made lakes. These dams regulate the normal flow of the river and control floods during normal rainy seasons. But unfortunately, due to weather pattern changes resulting from global warming and greenhouse effects, coupled with severe land degradation and de-afforestration in the Kenya highlands high floods occur frequently.

Dwars Heederik en Vertey (DHV) studied Lower Tana River morphology in 1986. The study analyzed the behavior of alluvial reaches, effects of various existing/future structures, and suitability of the river for navigation. They recommended study on prediction of floods by formulating a warning system in the Lower Tana River. This was deemed important to farmers and others. It was therefore necessary to study flood's behaviour to be able to effectively develop mitigation measures.

The impact following dam construction along the Tana River was studied by Maingi and Marsh (2002). Daily pre-dam and post-dam discharge data (1933 - 1996) of Garissa River Gauging Station was used. According to Maingi and Marsh (2002) there was little modification in the hydrologic regime of the Tana River since the construction of Masinga Dam in 1981. April-May floods have since declined by up to 22%, while November-December flows have remained virtually unchanged during the post-dam period. Therefore, there has been little effect on flood damage reduction downstream due to damming upstream. Previous environmental impact studies on dam construction across the Tana River have focused on the reservoir area and ignored the downstream impacts. This study on impact following dam construction along the Tana River had hoped to demonstrate that adverse environmental effects resulting from damming of the Tana River extend beyond the reservoir and therefore there is a need for future studies to address downstream effects as well.

Hydrology on the reforestation of the Upper Tana River Catchment and the Masinga Dam was studied by Jacobs et al (2004). Potential impact of unregulated deforestation and expansion of cultivation practices onto marginal soils in this critical

27

river basin involve significant reservoir siltation, reduced ecosystem function and more erratic downstream flows. The results of this study shows that full implementation of reforestation to an elevation of 1,850 m would result in a 7% decrease in sediment loading in the Masinga Reservoir. Runoff yields would be similar to baseline conditions but peak annual flows would increase by approximately 3% with less inter-annual variability and greater stability of water levels in the reservoir (Jacobs *et al*, 2004).

Mutua *et al* (2005) studied the prediction of annual sediment loading into Masinga Reservoir and the subsequent storage capacity reduction The designed sediment load into this reservoir in 1981 was estimated to be $3.0 \times 10^6 \, m^3$ per year (about 1% per annum reservoir reduction). By 2000, annual sediment loading had increased to over $11.0 \times 10^6 \, m^3$, nearly four times due to increasing land use change within Masinga catchment over the years and reduction in the designed capacity by more than 15%. There is need therefore to quantify spatially soil erosion and sediment yield reaching the reservoir with a view to reducing the sediment delivery. The study provided a comprehensive procedure by use of GIS supported soil erosion and sediment models for predicting spatial sediment yield and overall mean annual sediment volume delivered to Masinga reservoir. The study predicted that the annual sediment loading into the reservoir was about $14.0 \times 10^6 \, m^3$ for land use practices in 2003. However, according to the study by simulation of the best feasible management practices (BMPs), the achieved results show that the sediment volume reaching the reservoir could be reduced to about $6.0 \times 10^6 \, m^3$ per year.

Mutua and klik (2007) applied USGS Geospatial Stream Flow Model (SFM) to the Masinga catchment along Tana river in their prediction of daily streamflow in ungauged rural catchments. The results of this study gave a model performance coefficient of 0.74 based on the Nash-Sutcliffe statistical criterion.

2.13   Conceptual Framework

Floods account for the largest number of natural disasters and affect more people than any other types of natural disasters in many regions of the world. Heavy rainfall is the primary causative factor for floods in many temperate and tropical regions across the world. Most of the runoff that causes flooding in lower Tana plain is generated in the

upper Tana catchments which receive much higher rainfall than the plains in the downstream reaches. Flood related problems include loss of life, destruction of property, displacement of people, water logging, road network disruption, soil/river bank erosion, mass deposition of sand, health hazards (mosquito breeding) and environmental pollution. The inhabitants of North Eastern Province have learnt "to live with the floods". There is no flood control or flood protection in the study area. There is little or no viable economic and social coping mechanisms (preparedness, response and recovery measures) employed by the local community to protect and cope with the effects of the floods. No flood mitigation measures have been put in place and there is no flood warning system to provide time for evacuation and other measures.

Dwars Heederik en Vertey (DHV, 1986) studied behavior of alluvial reaches, effects of various existing/future structures, and suitability of the river for navigation between 1983 and 1986. They recommended study on prediction of floods by formulating a warning system in the Lower Tana River. The impact following dam construction along the Tana River was studied by Maingi and Marsh (2002). This study recommended that adverse environmental effects resulting from damming of the Tana River extend beyond the reservoir and therefore there is a need for future studies to address downstream effects as well. Mutua and klik (2007) applied USGS Geospatial Stream Flow Model (SFM) to the Masinga catchment along Tana river in their prediction of daily streamflow in ungauged rural catchments.

The broad objective for this study was to evaluate the magnitude of flood flow in Lower Tana to facilitate mitigation and adaptation measures, and economic use of the flood. Spatial semi- distributed United State Geological Survey - Stream Flow Model (USGS-SFM) was used in this study for developing non-structural (flood warning system) and structural (identifying flood diversion sites) mitigation measures. Structural measure (diversion) is an important element for purpose of focusing on the protection of human health and safety, and valuable goods and property. The proposed three inter-basin diversions from Tana to Ewaso Ng'iro Basin will reduce flood damage, open up more land (outside Tana valley) for irrigated food production, improve environment and develop water resources in this arid and semi-arid area. Flood warning system through forecasting provides some time for evacuation and other measures. Structural measure

(diversion) is an important element for purpose of focusing on the protection of human health and safety, and valuable goods and property. The proposed three inter-basin diversions from Tana to Ewaso Ng'iro Basin will reduce flood damage, open up more land (outside Tana valley) for irrigated food production, improve environment and develop water resources in this arid and semi-arid area.

CHAPTER 3

MATERIALS AND METHODS

3.1   Study Area

The study area is a stretch of about 400 km upstream of Garissa town along the riverine area of Lower Tana basin.   Three basins were used in this study. Two of these basins are in the lower and one in the middle Tana River.   The altitude of the study area varies from about 117 m in the flat flood prone area of Lower Tana to 4300 m (near Mount Kenya) above sea level in the Middle Tana Basin. It is located between 0^0 09' 53.3" South, 37^0 19' 16.15" East and 0^0 29' 48.79" South, 39^0 39' 17.32" East.
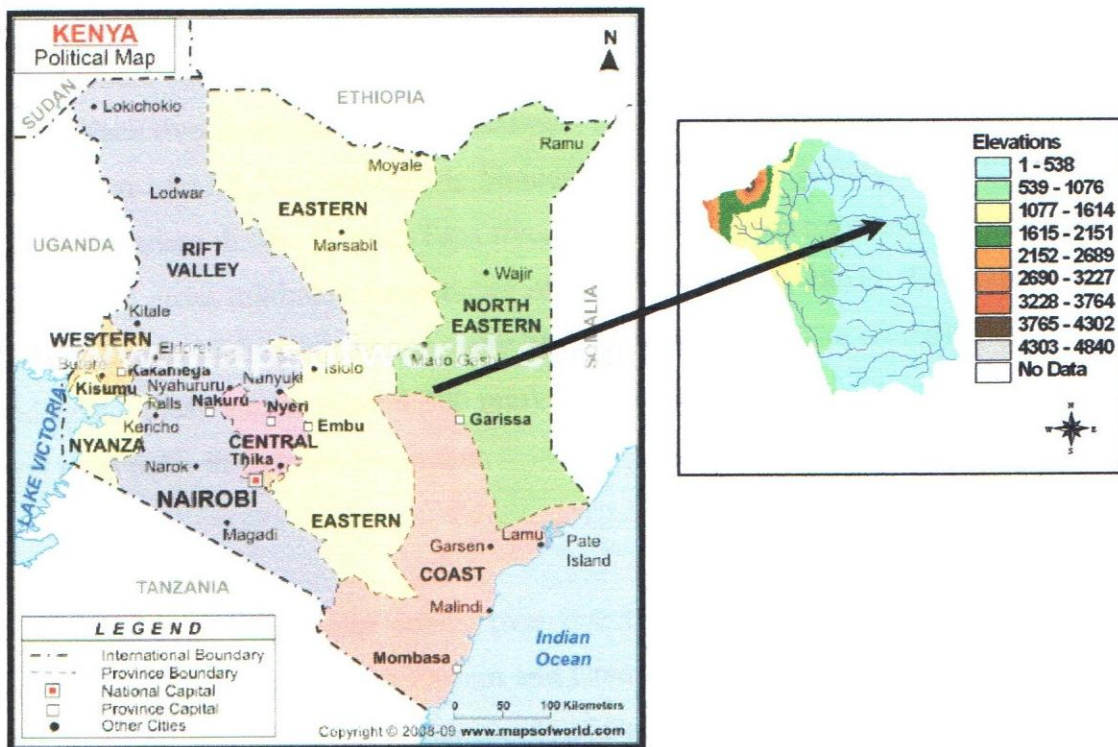
Source: Map of World, MapXL Inc, 2009

Figure 3.1: Study Area

3.1.1 Land Use and Land Cover

Tana Bain is divided into three catchments namely upper, middle and lower catchment areas (Agwata, 2006). The upper catchment covers about 15,000 km² at an altitude of 1000 m above mean sea level whilst the middle catchment covers an area of 15,700 km² at an altitude of between 1,000 and 200 meters above mean sea level. The lower catchment covers about 95,300 km² at altitudes below 200 meters (Hirji et al., 1996). There are horticultural, food crops and livestock production (milk) in various parts of Middle Tana Basin. In Lower Tana, especially around Garissa there are small irrigation schemes and riverine forest (0.5–3.0 km on either side) along the banks of the Tana river. Forest regeneration is lacking is section of Tana river (Maingi and Marsh, 2002).

3.1.2 Climate

Nearly 80% of the Tana basin is arid and semi arid and only 20% of the land is humid where rain fed agricultural production is practiced (Agwata, 2006). Meru in Middle Tana river basin has a mean maximum temperature of 25 °C and mean minimum temperature of 17.5 °C. Rainfall is bimodal and fluctuates between 500 to 800 mm annually. Garissa district (Lower Tana river basin) has a mean maximum temperature of 34.5 °C and mean minimum temperature of 32.4 °C (PDALE, 2003). Evaporation rates are high due to high temperatures (over 2600 mm per year). The rainfall is erratic and inadequate (mean annual rainfall-300 mm). The long rain occurs in April-May while the short rains come in October-December.

3.1.3 Demography

The Tana river basin covers over twenty districts in four different provinces namely Central, Eastern, North Eastern and Coast. It sustains a population of about five million people (Agwata, 2006). The people of Garissa district are predominantly Somali pastoralist. The population of Garissa district for 2003 was projected at 368,593 persons (excluding the 130,000 refugee population). Of the total population, 25% live in Garissa town, which acts as a safety net for those who lost their livestock during drought.

3.2   Data Requirement

Geo-information, meteorological and hydrological data were collected for the three basins along Tana River. Raw data were checked for missing ones and out-liars eliminated. One basin is in the middle and the other two basins are in Lower Tana River. This information was used in defining the aerial extent of the watershed being modeled, physical characteristics, precipitation falling, and moisture losses due to evapotranspiration in the simulation of the daily stream flow.

Data collected includes Digital Elevation Model (DEM), hydrologic network, land use, soils, ground and satellite daily precipitation and evaporation and ground daily gauged station stream flows.

3.2.1   Digital Elevation Model (DEM)

The shape-files which defined the three basins along Tana River were down loaded from the U.S. Geological Survey's National Center for EROS web-site. These African data are at HYDRO 1km grid. The model can also run on grids less than 1 km. In this study hydrological corrected DEM of 590 m resolution tar file in ARCINFO shapefile format was used as it gave hydrological stream network close to the actual ground situation.

Topographic Sheets from Survey of was also used in the identification of proposed potential flood water diversion sites. The sheets used are show in Table 3.1 below;

Table 3.1: Topo Sheets

Source	Sheet Number	Scale of Topo Sheet
Survey of Kenya	123-2	1:50,000
Survey of Kenya	124	1:50,000

3.2.2 Soil Data

Digital Soil Map of the World (DSMW) CD produced by FAO (United Nation's Food and Agriculture Organization) and UNESCO (United Nation's Educational, Scientific and Cultural Organization) was used. This data was acquired through Regional Centre for Mapping of Resources for Development, Nairobi, Kenya. This map is the finest resolution soil database with global coverage available. The data are in geographic projection and are produced from original map sheets with a scale of 1:5,000,000. This grid data was added to the Arc View project for use in the model.

3.2.3 Land Cover and Land Use Data

The Africa land cover characteristics data base can be downloaded from the U.S. Geological Survey's National Center for Earth Resources Observation Science (EROS) at http://edcdaac.usgs.gov/glcc/glcc.asp. This grid land cover and land use data were acquired through Regional Centre for Mapping of Resources for Development, Nairobi, Kenya.

3.2.4 Rainfall and Evaporation Data

Both daily grid Potential Evapotranspiration (PET) estimates and rainfall estimates (RFE) and meteorological ground station rainfall data were used in this study. NOAA's Climate Prediction Center produces daily grid rainfall estimates (RFE) for Africa since 1995. This PET and RFE data (1995 - 2006) were acquired through Regional Centre for Mapping of Resources for Development, Nairobi, Kenya as shown in Table 3.2 below;

Table 3.2: Satellite Potential Evapotranspiration (PET) and rainfall estimates (RFE)

Data	Year
Potential Evapotranspiration (PET)	2001 - 2006
Rainfall estimates (RFE)	1995 - 2006

Daily meteorological ground rainfall data (1970 - 2006) were acquired for Meru, Chuka, Embu, Materi and Garissa Station from Meteorological Department, Dagoreti, Nairobi. Details are given in Table 3.3;

34

Table 3.3: Ground rainfall

Station	Station ID	Daily Data	Year	% Missing Data
Meru	8937065	Rainfall	1970 - 2006	0
Chuka	9037034	Rainfall	1972 - 1989	0
Embu	9037202	Rainfall	1976 - 2006	0
Materi	9037200	Rainfall	1976 - 2001	0
Garissa	9039000	Rainfall	1970 - 2006	0

3.2.5 Hydrological Data

Daily flows data of 25 gauging stations along Tana River were collected from Ministry of Water and Irrigation's Maji House and Garissa Station. These stations are Mutonga (4EA01), Mutonga (4EA06), Mutonga Kamarandi Primary School (4EA07), Nthi (4EB01), Thuchi (4EB04), Rugutii (4EB05), Rugutu (4EB06), Thuchi (4EB07), Tungu (4EB09), Mara (4EB11), Ena (4EC03), Thingishu(New)(4F04), Mariara(New) (4F05), Gatabora (4F06), Thangatha (4F08), Ura(New) (4F09), Kazita (4F10), Tana at Grandfall(4F13), Thingithu (4F17), Kazita (4F19), Tana At Garissa (4G01), Tana at Garsene (4G02), Tana at Korakora(4G06), Tana at Saka (4G010) and Tana at Nanighi (4G08). The stations are arranged in series.

Most gauging stations have many missing daily flow data after 1994 and most only operated for a short period of time. Only Kazita (4F19), Grand Fall (4F13) and Garissa (4G1) were used in this study as their data are consistent between 1980 and 1988. These selected stations are situated at strategic points in the three basins used in this study (Table 3.4).

Table 3.4: Gauging Stations

Station Number	Station Name	Date Installed	Year	% Missing Data
4 F 19	Kazita	1966	1980 - 82	3.19
			1986 - 88	2.09
4 F 13	Grand Falls	1962	1986 - 88	4.47
4 G 1	Garissa	1933	1986 - 88	3.47

Source: Ministry of Water Development, 1992

3.3 Data Processing

The model uses topography, soil and land cover/use data in its parameterization. It has geographical user interface (GUI) for input data preparation and output visualization. It combines Rainfall – Runoff and Flow Routing models in the water balance, routing and forecasting modules of the model.

3.3.1 Terrain Analysis

Each basin was modeled separately. The basin under investigation was selected from Africa data and is initially converted to shape-file. Hydro-DEM from Africa data base was added to the existing shape-file's view. The boundaries for each basin were extracted using the given African hydro-DEM and grid converted shape-files. The final extracted files were analyzed and some map calculations to produce a corrected elevations grid was done. Through the model's tool, the sinks of the corrected elevations grid of the map calculation's DEM were filled to avoid negative values. Terrain analysis function divided the study area into smaller sub-basin and rivers, establish the connectivity between these elements and computes topography dependent parameters of the model. Flow direction, flow accumulation, flow length, streams–grid, stream links, outlets–grid, basins–grid, hill slope length–grid, terrain slope–grid and downstream ordering–grid themes were created. Flow direction grid paved the way for the determination of upstream contributing area, distance to the basin outlet, and the slope of the land surface. These created grids under terrain analysis were was used as input files for parameter estimation, generation of unit hydrograph response and other modules of the model.

3.3.2 Parameter Estimation

The quantity of simulated surface runoff in a river basin due to a rainfall event depends very heavily on the nature and condition of underlying soils, land cover and slopes (Artan *et al*, 2001). USGS Stream Flow Model contains algorithms for estimating flow simulation parameters for each catchment and river reach from land cover and soil data sets (Asante *et al*, 2008). These parameters included soil water holding capacity,

36

hydrological active soil depth, texture, average saturated hydraulic conductivity, Soil Conservation Service (SCS) runoff curve number and percentage of impervious cover.

The FAO soils data set specifies the top and bottom depths and the percentage of the texture type (sand, silt, and clay) of soil horizons in 106 different soil types cataloged for nine regions (Asante *et al*, 2008). The FAO soil depth categories are shown on Table 3.2 below;

Table 3.5: FAO Soils Depth Class

Depth Category	Range of depth	Median soil depth
Very Shallow	< 10 cm	5 cm
Shallow	10 – 50 cm	30 cm
Moderately Deep	50 – 100 cm	75 cm
Deep	100 – 150 cm	125 cm
Very Deep	100 –300 cm	200 cm

Source: Artan *et al*, 2001

The model estimated the average soil depth by adding percentage of very shallow, shallow, moderately deep, deep and very deep. It is assumed that the coarse soils in the FAO database relate to sandy soils, the medium soils are loamy soils, and the heavy soils are clay soils (Artan *et al*, 2001). FAO database contains a file "TEXTURE.ASC" that uses "1" to identify sandy soils, "2" to identify loamy soils, and "3" to identify clay soils. Estimated soil texture also by adding percentage of coarse, medium and clay. The model interface uses a grid of hydraulic conductivities to estimate the average hydraulic conductivity for each sub-watershed within the watershed being modeled (Artan *et al*, 2001). The estimate for average saturation soil hydraulic conductivity (HC_{ass}) based upon the soil texture computation for each sub-watershed was given by;

$$HC_{ass} = (P_{c(s)}) * 0.001) + (P_{m(l)}) * 0.0001) + (P_{h(c)} * 0.0000001) \qquad (3.1)$$

where $P_{c(s)}$ is percent coarse (sand), $P_{m(l)}$ is percent medium (loamy) and $P_{h(c)}$ is percent heavy (clay).

The estimated soil's hydraulic conductivity, maximum impervious ground cover, curve number, soil, texture, and water holding capacity data were added to the ArcView projection as grid for use in the model.

The soil and land cover data sets were used together to determine Soil Conservation Service (SCS) runoff curve numbers. The curve numbers were used in the determination of amount of rainfall that changed to surface runoff. The curve numbers were assigned based on land cover type and the soil hydraulic classes of the U.S. Department of Agriculture's (USDA) soil classification system (Asante *et al*, 2008). The coarse and medium/coarse textures in the FAO data set are matched with the loam and sandy loam (USDA group A) classes. Likewise, medium and medium/fine FAO classes are matched to the USDA soil classes B and C respectively while FAO fine class is matched to the USDA class D. The intersection of the land cover and soil texture grids yields a runoff curve number.

After running these parameters using the model, three text files were generated describing each sub-basin. These were basins (basin characteristic), file-order (step to be followed in running the model) and river (river characteristics) text files were later used by the model to generate simulated daily stream flow. These estimated data were used later in the model for developing simulated surface runoff, flow velocity and attenuation parameters in each sub-basin.

3.3.3 Generation of Unit Hydrograph Response

The nature of land cover and land use influences runoff generation and overland flow processes. A unit hydrograph was developed to simulate the typical response of the catchment to a uniformly distributed water input event. Model contains automated GIS based algorithms for generating these responses (Artan *et al*, 2001). The default procedure began by the estimation of uniform overland velocity for each catchment based on the mean slope of the catchment and dominant land cover type present. The distance along the flow path from each grid cell in the catchment to the catchment outlet was also computed. The travel time from each grid cell to the catchment outlet was also computed using flow length and travel time. The distribution of discharge at the catchment outlet was given by the probability density function (PDF) of travel times in the catchment. The unit hydrograph or probability mass function of flow travel times was obtained by discretizing the PDF over the routing interval of a day. The unit hydrograph response was

computed for each catchment during preprocessing and stored in an ASCII file for subsequent use. Together with soils data, land cover and land use data parameters were used to determine the response coefficients for determining the sub-basin water balance (amount of excess precipitation, recharge to the ground-water system, and water held in storage in the soils).

3.3.4 Generation of Rainfall and Evapotranspiration Data

Both daily grid rainfall estimates (RFE) and meteorological station rainfall data were used in this study. The USGS-SFM model was used through its methods for spatial integration of the RFE over topologically linked river sub-basins derived from DEM. The model generated annual daily RFE for the years 1995 to 2006 for each sub-basin in the three basins separately in the forms of excel text from the grid format. The generated annual daily RFE data for the years (1995-2006) together with other parameter were able to create daily stream flow simulations for the same period. However, the daily actual ground data of gauging stations of Tana River from 1995 to 2006 were either lacking or in some stations having many missing data. As an example, Garissa Station (4G1) along Tana River has consistent data from 1948 to 1992. After 1994 there were no data collected at Garissa Station (4G1). Only Kazita (4F19), Grand Fall (4F13) and Garissa (4G1) river gauging station were used in this study as their data are consistent between 1980 and 1988. Therefore, the rainfall from 1980 to 1988 was generated for each sub-basin of the three basins on annual basis. The distribution of ground meteorological station is wide. The distance between those existing ground stations with good data is more than 100 km. The RFE has a spatial and quantitative distribution of 8-kilometers resolution and there is data for each sub-basin. Therefore, it was necessary to use the generated RFE grids on annual basis for the entire sub-basin for each of the three basins through interpolation method. These grids generated rain text file acted as an input file for flow routing. The generated daily RFE of 1995 -2006 for Meru and Garissa at sub-basin level were compared with actual daily ground meteorological station data for the purpose of determining their correlations. Also the correlations of generated daily RFE (1995-2006) at each basin level for each sub-basin to sub-basin relationship were determined. This assisted in generation of daily estimated ground rainfall for sub-basins

39

with no meteorological station by using data of exiting sub-basin's ground meteorological stations in the same basin. Through these correlations and interpolations, the existing ground station daily rainfall data was used at basin level to generate daily rainfall estimate (ground) for the years 1980 to 1988 for each sub-basin. This rainfall data was interpolated into site-specific precipitation by model's grid theme as input-data files for simulation of daily stream-flow.

The grid for potential evapotranspiration (PET) for the model has been generated by Global Data Assimilation System (GDAS) through the use of Penman-Monteith equation at a daily time step. The model ingested the resulting PET grids and computed actual daily evapotranspiration from 2001 to 2006 based on antecedent soil moisture conditions. The daily PET for all sub-basins were prepared based on the average daily data of 2001 – 2006.

3.4   Simulation of Daily Stream Flow

The soil water balance module separated input rainfall into evapotranspiration, surface run-off, interflow, base-flow and ground water components. It provided and also maintained an accounting of water in storage (soil moisture content) at the end of each simulation time step of the model.

3.4.1   Computation of Soil Water Balance

The soil parameters used by the model in computing soil moisture conditions on a daily basis were hydraulic conductivity, maximum impervious ground cover, curve number, soil, texture, and water holding capacity. The control soil column volume was modeled as two layer soil (top soil is 10%) with rainfall as the only input and evapotranspiration, surface runoff, interflow and base flow. processes and deep ground water percolation as outputs.

The rain, evaporation, basin characteristic and response text files were the main input for determination of water balance. The curve number was used in separating runoff into surface and interflow components while the Green-Ampt equation extracted water from the interflow soil layer to feed the base flow soil layer. Finally the model generated output files containing the fluxes from the respective surface, interflow, base flow and

40

deep percolation phases of flow as well as the soil moisture storage. The output files generated by the model were used in the next stage of water routing inside the watershed and channel.

3.5   Routing Water inside the Watershed

The model used basin run-off yield, response and river text files created during computation of basin characteristic and water balance modules in the routing of water inside the watershed. Basin characteristic file included the inputs of river text file included channel's manning coefficient, length, mean slope and mean width. Direct surface runoff, interflow, and base flow were added to their respective linear reservoirs and the quantity of water routed to the respective reservoirs associated with the downstream watershed subtracted out as show by Figure 3.2.
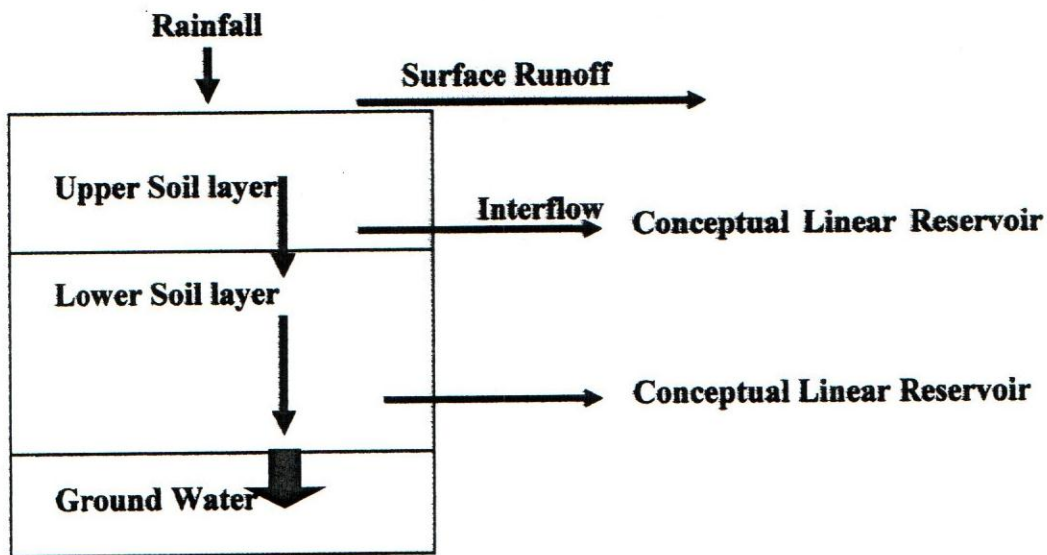
Figure 3.2: Transferring Fluxes in two layered model

Routing of excess precipitation and water in the stream channel was done using lag coefficients (Artan *et al*, 2001). It is based on the Soil Conservation Service (SCS) Curve Number method. This method takes into account vegetation, soil type, and antecedent moisture, was used for separating runoff into surface and interflow components (Asamte *et al*, 2008).

$$LF = ((L^{0.8} * ((1000/CN) - 9)^{0.7}) / (31.67 * S_a^{0.5})) / (60 * \Delta t) \qquad (3.2)$$

41

where *LF* is lag factor, *L* is Length, S_a is average slope, *CN* is curve number and Δt is time step. The total runoff (Q_t) from within the watershed was computed as;

$$Q_t = ((SR_d + IF + BF)* (watershed\ area\ *\ 1000)) / (\Delta t*3600) \qquad (3.3)$$

where SR_d direct surface runoff, *IF* is inter flow and *BF* is base flow.

3.6   Channel Flow Routing

The model uses Muskingum-Cunge, diffusion analogy and simple lag methods in channel flow routing. Muskingum-Cunge Channel routing method has been used for routing the water down the channel. The main input files for the model's channel routing included river text with channel's manning coefficient, length, mean slope and mean width. The other inputs files included in-stream infiltration and evaporation water loss fraction, landform (mean length of the mainstream tributaries, basin area and basin outlet upstream watershed area), river routing parameters (Muskingum Cunge routing scheme coefficients, number of segments in a reach, number of routing interval per time step, routing segment length, initial streamflow, travel for water passing through channel segment and celerity of the flow).

The flow routing starts with the most upstream watershed and estimates the initial stream-flow as being the stream-flow needed to achieve a bank full condition (Artan *et al*, 2001). Bank full stream-flow was estimated by;

$$Q = (0.3 * (3.7 * (A_{aws}/ 2.59)^{1.15}) * (S_a)^{0.23}) /3 \qquad (3.4)$$

where A_{aws} is total area above the watershed outflow and S_a is average channel slope. The model executes a loop to compute the Muskingum weighting coefficient. The coefficient must be less than 0.0001 or greater than 0.5 using the formula;

$$K = \Delta X / C$$

$$X = 1/2\ [\ 1 - Q / B\ S_o C\ \Delta X\ ]$$

where *K* is Muskingum proportionality coefficient, *X* is Muskingum weighing coefficient and ΔX is space step. The number of subdivisions in a channel was computed as;

Channel subdivisions = channel length / ΔX

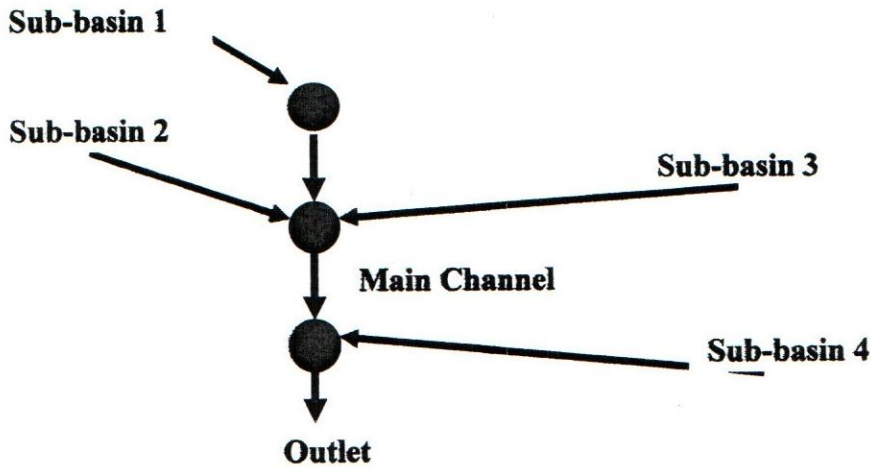Figure 3.3 shows the river network in channel routing.

Figure 3.3: Channel Routing

For propagation of flow within the river channel, a set of Muskingum coefficients were computed using the four coefficients in equations (2.15 - 2.18). The stream-flow at each space step/time step was saved and used as the initial condition at the next time step. The stream-flow at the next space step was computed as;

Stream-flow at the watershed's outlet = (C_0 * Discharge at previous space step) + (C_1 * Discharge at previous space step at the previous time step) + (C_2 * Discharge at the current space step at previous time step) + C_4 (Q_L).

3.7   Calibration and Validation

USGS-Stream Flow Model was calibrated and validated by assessment of the goodness of fit between the simulated and observed stream-flow data at Kazita (F19), Grand Falls (4F13) and Garissa (4G1) stations. The model does calibration and validation by the use of monthly and annual flow statistics series. The sensitivity analysis was used to test which parameters were to be used for calibration and their feasible ranges. It measured the impact on the model outputs due to changes in the model inputs. The sensitivity analysis of twenty parameters was done using the model for the purpose of

43

determining the most sensitive. The model was calibrated using Meru sub-basin's Kazita (F19) station in the Middle Tana River basin.

Kazita (F19) station's daily ground data of 1980 to 1982 were used because flood during this period had few missing data. These data were converted to annual texture files for use by the model in automatic calibration. However, the automatic calibration process of the model did not work out for lack of algorithm. Therefore, manual calibration was use.

The model simulated daily stream based on water balance principle of separating the only input rainfall (precipitation) into evapotranspiration, surface run-off, interflow, base-flow and ground water components at the end of each time step. For the days with no rainfall, the result was zero simulated stream flow (generated by the model). The stream was carrying the normal base flow at these times of zero rainfall. The observed ground daily stream-flow data of Kazita (F19) station for 1980 to 1982 was separated into daily base-flow and flow caused by surface run-off from rainfall effects. This separation of base-flow was done by the use of semi-log graph paper. The annual daily base flow data were converted into natural $\log_e$ (ln) and used against time (1 year). A time step of 1 day was used. The points in a straight line assisted in determining average base flow for that section of the graph. The actual surface run-off (caused by the rainfall) component that contributed to the stream flow on daily bases was determined by subtracting observed daily flow from the corresponding daily base flow.

The correlation of annual daily simulated and observed stream-flow data of Kazita (F19) for the 1980 to 1982 was tested initially before any calibration for all flows (low and high flows). The initial results indicated that calibration was necessary for higher correlation coefficients (R^2) to be created. The most sensitive parameters determined by the models sensitivity analysis component included soil water holding capacity, soil depth, runoff curve number and pan evapotranspiration (PET) loss correction. These were the parameters used in calibration process. One-at-a-time per parameter method was used, where the model was run manual each time with only one parameter changed (within a range) many times while all other parameters were held constant.

The parameter which gave the highest values correlation coefficients (R^2)

between annual daily simulated and observed stream-flow was selected. In this case Pan Coefficient for Evapo-transpiration loss correction was calibrated with an adjustment of 15% before simulation of these daily stream flows (1980-82) at Kazita Station (4F19). The same data was further tried for goodness of fit by use of Nash *et al* (1970) equation (2.27) to reduce the overall uncertainty of simulation. The result was 0.8, hence a good fit. The performance of the model is above average.

After the model was calibrated with plausible parameter values, the model was validated using the same adjusted parameter in calibration. The idea was to ensure that it can be used for prediction. In the validation process, the model was tested against Kazita (F19) and Garissa (4G1) ground gauging station with daily annual observed stream flow data for 1986-88 years. The observed ground daily annual stream-flow data of Kazita (F19) and Garissa (4G1) ground gauging station for 1986 to 1988 was separated in the same process as stated above into daily base-flow and flow caused by surface run-off from rainfall effects. A correlation was determined between annual daily simulated and observed stream-flow for each of these two stations for 1986-88 period.

3.8   Stream Flow Forecasting

The model can do short period/lead time of 1 to 3 forecasting of flood between stream gauging stations. Peak flood was put into steady gradually varied channel geometry in order to forecast flood level at points down stream. The model was made to run up to three days before the peak flow for generation of forecasted stream flow.

3.9   Updating Bank-full and Flow Statistics (Post-Processing)

The model used streamflow.txt parameter as the input file and monthlyflow.txt and annualflow.txt as default output files. The model processed input file and gave a final updated output riverstats.txt with statistical estimate of carrying capacity (how much water is needed to fill a river) of channels or streams in every sub-basin. Any flow stream or river flow above maximum or bank-full is assumed to be flood flow.

3.10 Flood Magnitude at Proposed Diversion Sites

Eastern Ewaso Ng'iro River Watershed comes close to Tana River basin (about 15 km) upstream of Mbalambala town (PPO NEP, 2003). They are ideal sites for construction of diversion channels to carry away some of the excess flood water from Tana River to Ewaso Ng'iro plains. Three ideal points were identified based on the use of sub-basin physical features generated by the model's complete terrain analysis function and contours from the topo-maps as possible potential sites for diversions. The possibility of water flowing through diversion channels between the two basins depended on the topographical difference between the proposed outlet from Tana River and inlet at Ewaso Ng'iro Basin. Contours assisted in determining the course for each diversion channel.

Magnitude of flood flow at these three ungauged proposed potential diversion sites were determined by use of the daily base stream flow of Grand Fall Station (F13) and the validated daily stream flow simulated by the model for the Tana Basin A and Tana Basin B. The position of Grand Fall Station (F13) is the most upstream starting point of Tana Basin A. The daily stream flow data for years 1986 – 1988 were used in the generation of these estimated daily stream flow for the three proposed potential site. River daily flows above bank-full (maximum) for these three proposed potential diversion site were assumed to be flood flows.

CHAPTER 4

RESULTS AND DISCUSSIONS

4.1   Tana Basins

The study covered three adjacent basins of Tana River. These were referred to Tana Basin A, Tana Basin B and Tana Basin C in this study (names for this study only). Each basin has many sub-basins. Tana Basin A is located in mid Tana Basin and other two basins are in the lower Tana flood plains. The position of the three basins within the whole Tana River Basin is shown below in Figure 4.1;
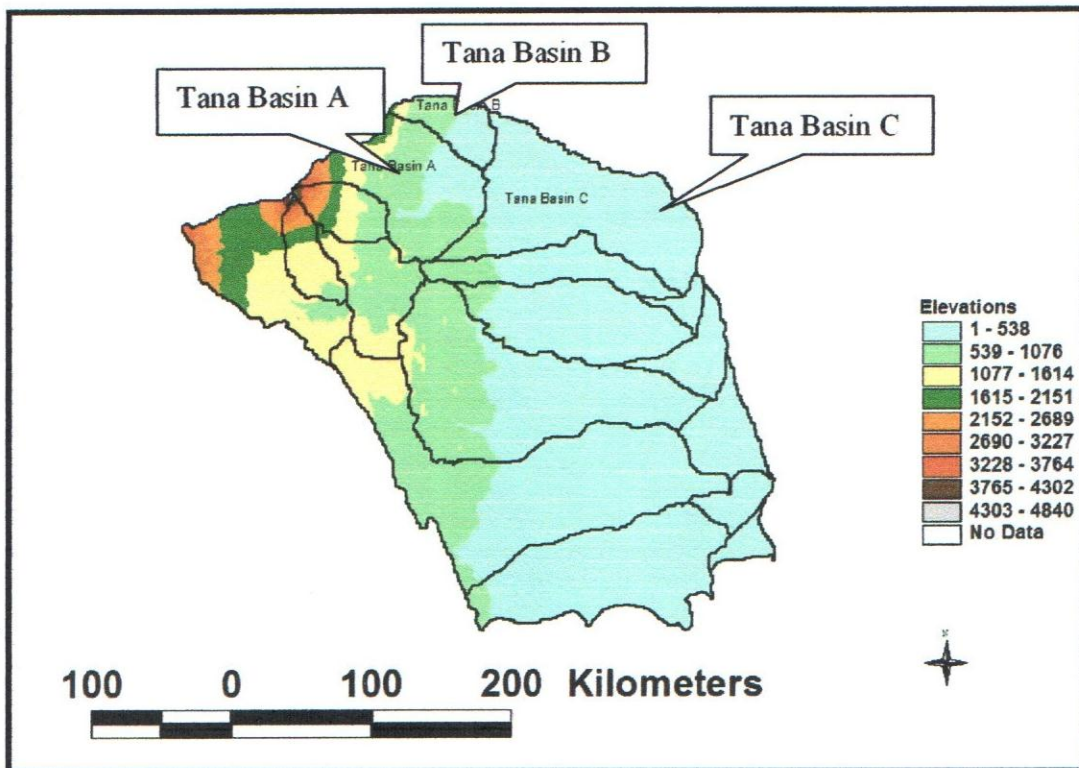

Figure 4.1: Map of whole Tana River Basin

Figure 4.2 shows the map of Tana Basin A with 11 sub-basins. The total area of this basin was 6,686.9 km^2 (see Table 4.1). Observed daily rainfall data for the years 1995-2006 were compared with Satellite rainfall estimate (RFE) in Tana Basins A (Meru) for the purpose of creating a relationship (estimating ground rainfall for sub-basins with

no meteorological stations). Tana Basin A has Meru meteorological station and Kazita Gauging station (4F19). Calibration was done in Tana Basin A with the use of sub-basin 8's observed and simulated daily stream flow data of 1980 – 82 at Kazita Gauging station (4F19). Also validation was done at the same station 4F19 and Garissa station (4G1)'s daily observed and simulated data of 1986 – 1988. These simulated flows were used in estimating flood flows at the three proposed potential flood water diversion sites. River flows above bank-full were assumed to be flood flows.
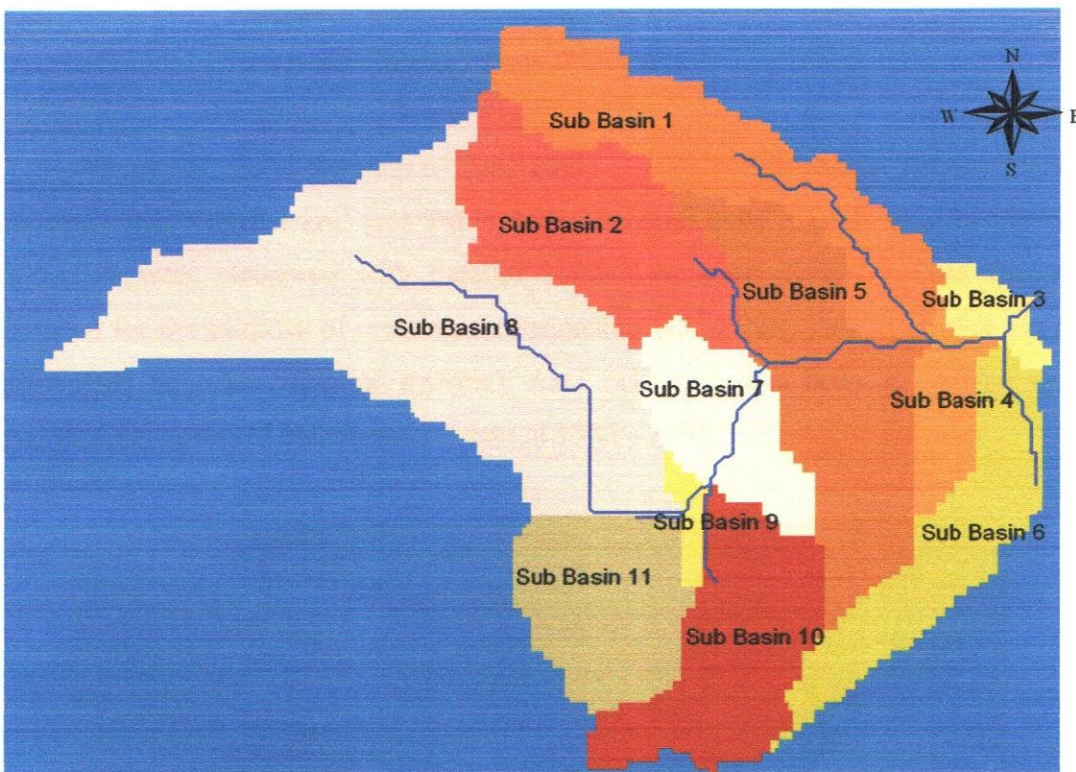

Figure 4.2: Map of Tana Basin A

Figure 4.3 shows the map of Tana Basin B with 3 sub-basins. The total area of this basin was 1,850.5 km^2 (see Table 4.2). It is located between the two other basins. This basin contributed some amount daily flow to the Tana river network. These daily flows were used in the validation of the model at Garissa Gauging Station (4G1).
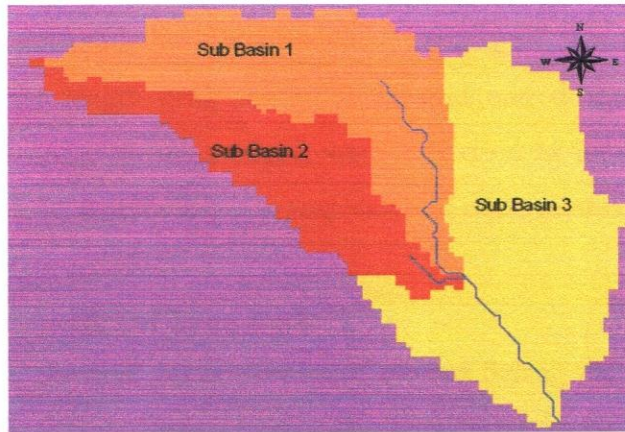
Figure 4.3: Map of Tana Basin B

Figure 4.4 shows the map of Tana Basin C with 15 sub-basins. The total area of this basin was 10,918.4 km^2 (see Table 4.3). Observed daily rainfall data for the years 1995-2006 were compared with Satellite rainfall estimate (RFE) in Tana Basins C (Garissa) for the purpose of creating a relationship (estimating ground rainfall for sub-basins with no meteorological stations). Also validation was done at Garissa station (4G1)'s daily observed and simulated data of 1986 – 1988.
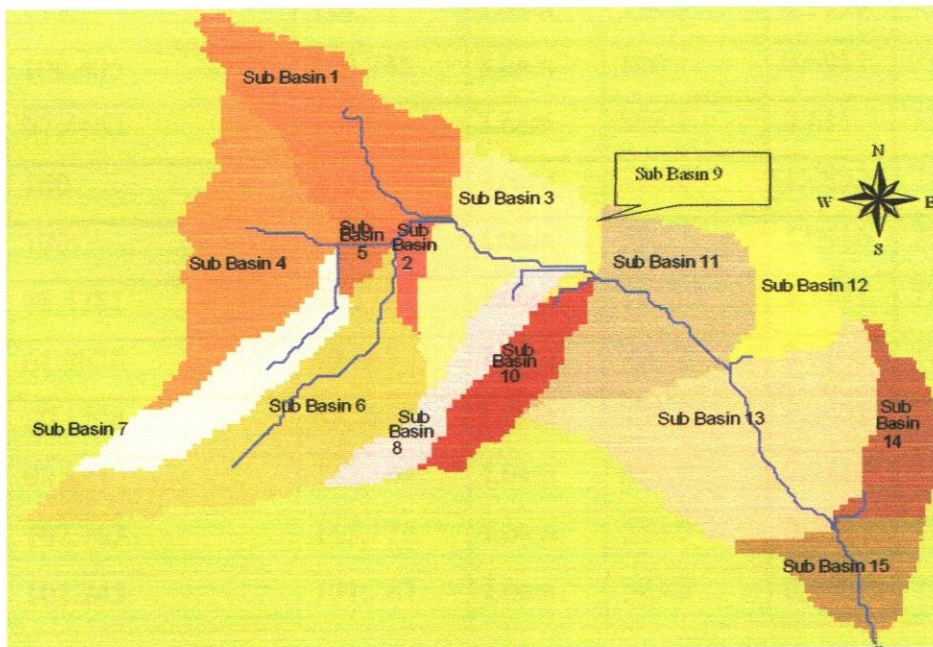

Figure 4.4: Tana Basin C

49

4.2 Terrain Analysis

The model performed terrain analysis for the three basins separately, generated flow direction, flow accumulation, flow length, streams–grid, stream links, outlets–grid, basins–grid, hill slope length–grid, terrain slope–grid and downstream ordering–grid themes. These grids under terrain analysis were was used as input files for parameter estimation, generation of unit hydrograph response and other modules of the model.

4.2.1 Physical Parameters of Tana Basin A

These basin's physical parameters were created during the parameter estimation module of the USGS Stream Flow Model. The parameters included soil water holding capacity, hydrological active soil depth, texture, hill slope, average saturated hydraulic conductivity, soil conservation service (SCS) runoff curve number and percentage of impervious cover. Table 4.1show the main physical parameters of Tana Basin A.

Table 4.1: Physical Parameters of Tana Basin A

Basin ID	Soil Water Holding Capacity (mm)	Soil Depth (cm)	Texture	Area (km²)	Hill Slope	Runoff Curve Number
3	113.3	121.55	Loam	114.9	0.5939	73.6
4	100.405	113.745	Loam	196	0.6951	73.2
5	97.4163	109.93	Loam	852.1	0.611	73.6
7	100	113.5	Loam	390.2	1.0833	73.5
9	100	113.5	Loam	59.5	1.0416	73
8	88.4281	97.1771	Loam	1850.5	1.3171	73.5
1	61.9678	59.887	Loam	790.2	0.9165	70.8
2	70.1708	85.3824	Loam	733.8	1.2452	72.3
10	98.821	112.144	Loam	637.7	0.9418	73.9
6	102.763	115.173	Loam	538.5	0.6541	75.3
11	102.245	131.287	Loam	523.5	0.8096	72

50

Figure 4.5 shows the general elevation of Tana Basin A. These basin's general elevation were number created during the terrain analysis module of the USGS Stream Flow Model.Highest areas for the sub-basins were near Mt. Kenya area and the lowest along the Tana River. All individual sub-basin inter-flow and surface run-off flow ended up in the Tana River.
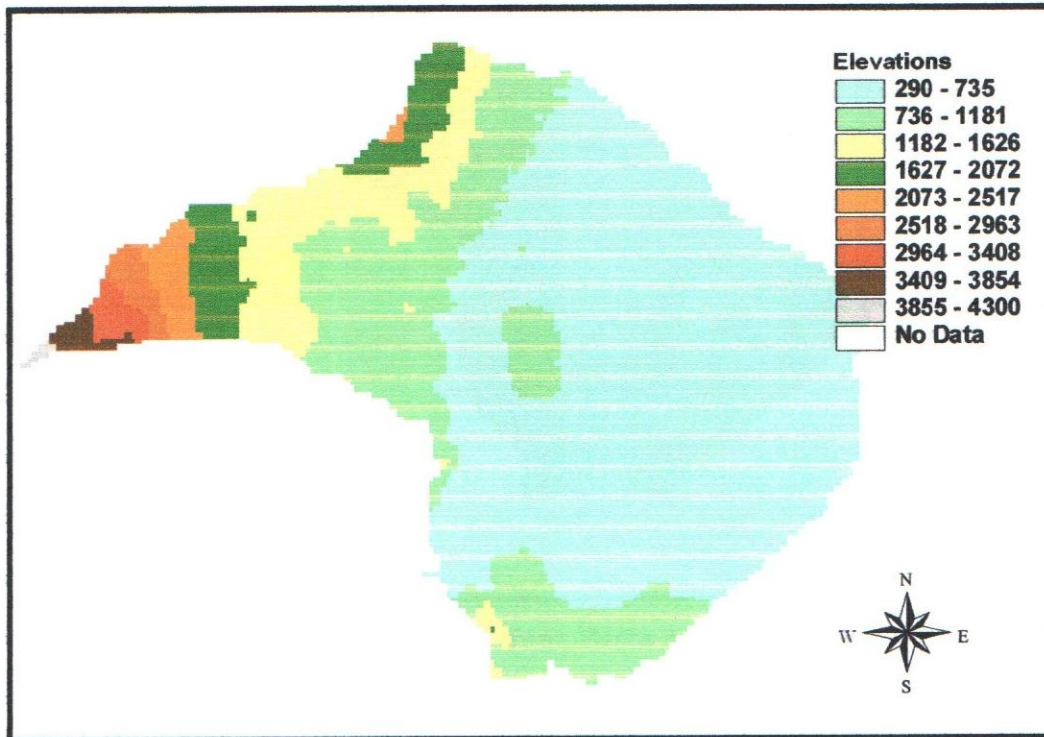

Figure 4.5: Elevation Tana Basin A (in meters)

Figure 4.6 shows the runoff curve number for Tana Basin A. This basin's runoff curve number were created during the parameter estimation module of the USGS Stream Flow Model. Highest runoff curve number for the sub-basins was 75.5 and the lowest 70.8. along the Tana River. The sub-basins have very close runoff curve number due to the fact that the soil group, land use and hydrological condtions were almost the same for all of them. In general lower numbers indicate low surface runoff potential while larger numbers are for increasing surface runoff potential. Therefore, predictions of direct surface runoff or infiltration from rainfall excess were almost the same for all the sub-basins.
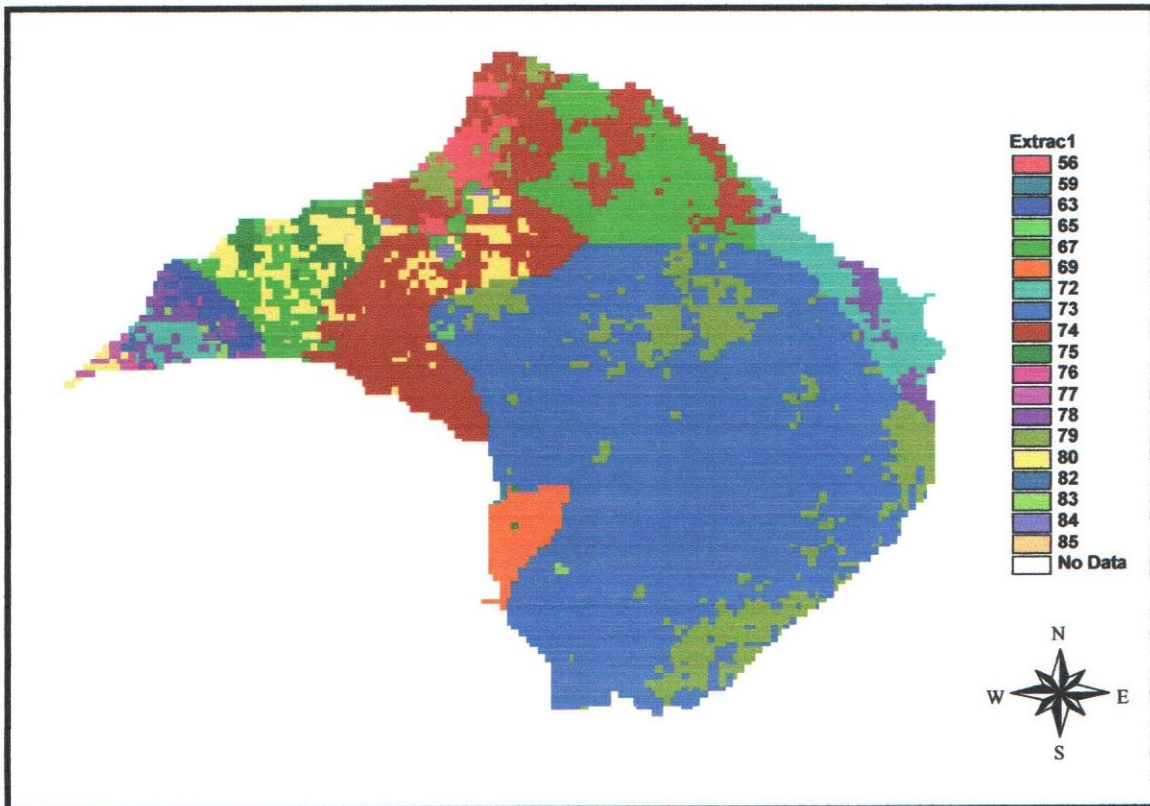
Figure 4.6: Runoff Curve Number for Tana Basin A

Figure 4.7 shows the soil depth for Tana Basin A. This basin's soil depth were created during the parameter estimation module of the USGS Stream Flow Model. Highest soil depth for the sub-basins was 131.3 cm and the lowest 59.9 cm along the Tana River. The realtionship of runoff curve number and soil depth for each individaul sub-basin were close. The sub-basin with lowest runoff curve number (70.8) is the same one with lowest soil depth (59.9 cm) and the same were almost true for other basin.
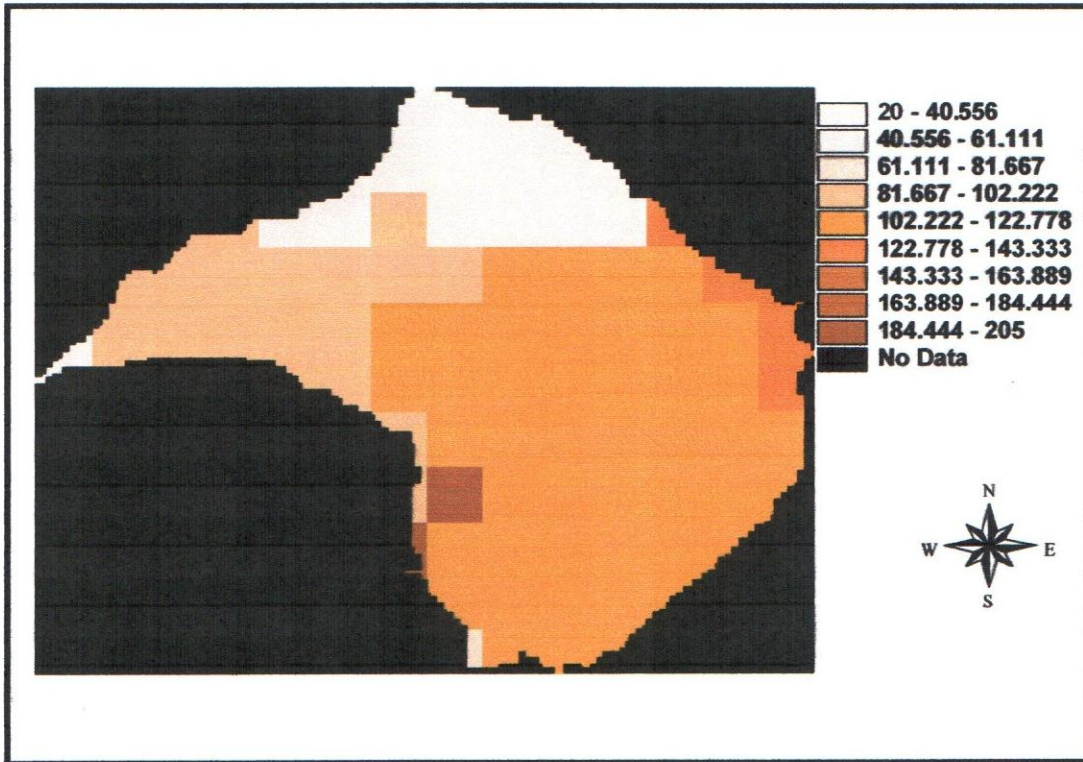
Figure 4.7: Soil Depth for Tana Basin A (in centimetres)

Figure 4.8 shows the soil water holding capacity for Tana Basin A. This basin's soil water holding capacity were created during the parameter estimation module of the USGS Stream Flow Model. Highest soil water holding capacity for the sub-basins was 113.3 mm and the lowest 61.97 mm along the Tana River. The realtionship of runoff number curve, soil depth and soil water holding capacity for each individaul sub-basin were close. The sub-basin with lowest runoff curve number (70.8) and soil depth (59.9 cm) is the same one with lowest soil water holding capacity (61.97 mm) and the same were almost true for other basin. The sub-basin final surface runoff is also affected by slope and surface area.
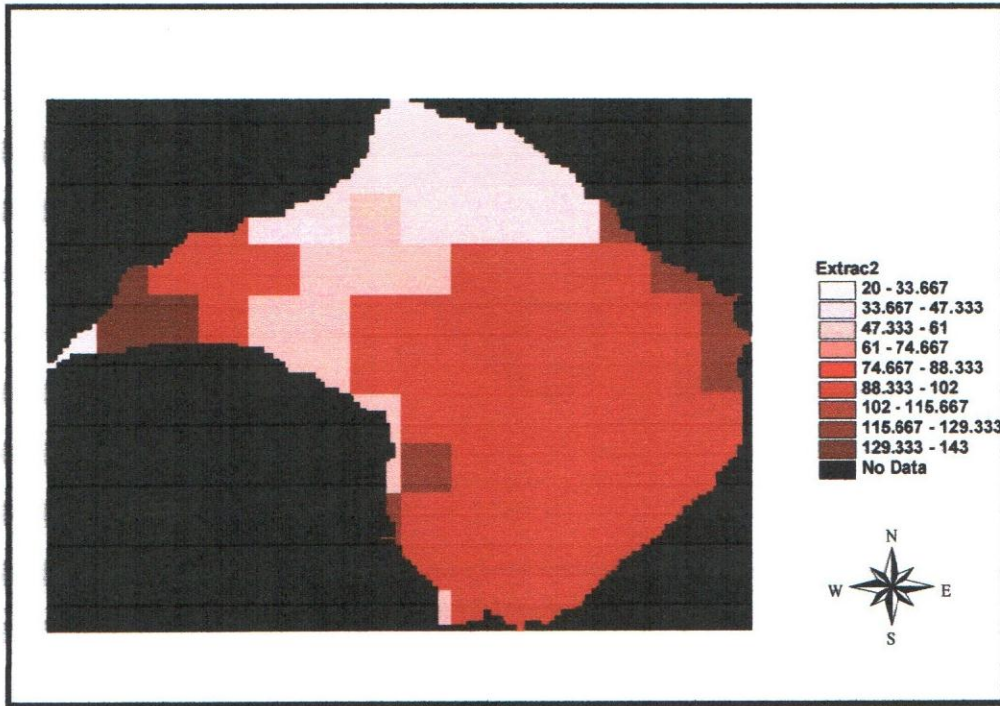
Figure 4.8: Soil Water Holding Capacity for Tana Basin A (in millimetre)

4.2.2 Physical Parameters of Tana Basin B

Below are table and figure indicating physical parameters for each sub-basin in Tana Basin B;

Table 4.2: Physical Parameters of Tana Basin B

Basin ID	Soil Water Holding Capacity (mm)	Soil Depth (cm)	Texture	Area (km^2)	Hill Slope	Runoff Curve Number
3	118.992	124.995	Loam	830.2	0.4772	73.5
1	107.69	111.627	Loam	608.1	0.749	72.2
2	88.4361	88.8603	Loam	422.2	0.9299	72.8

Figure 4.9 shows the general elevation of Tana Basin B. Highest areas for the sub-basins were near Mt. Kenya area and the lowest along the Tana River. All individual sub-basin inter-flow and surface run-off flow ended up in the Tana River.

Figure 4.9: Elevation Tana Basin B (in meters)

Figure 4.10 shows the runoff curve number for Tana Basin B. Highest runoff curve number for the sub-basins was 73.5 and the lowest 72.2 along the Tana River. The sub-basins have very close runoff number curve due to the fact that the soil group, land use and hydrological condtios were almost the same for all of them.
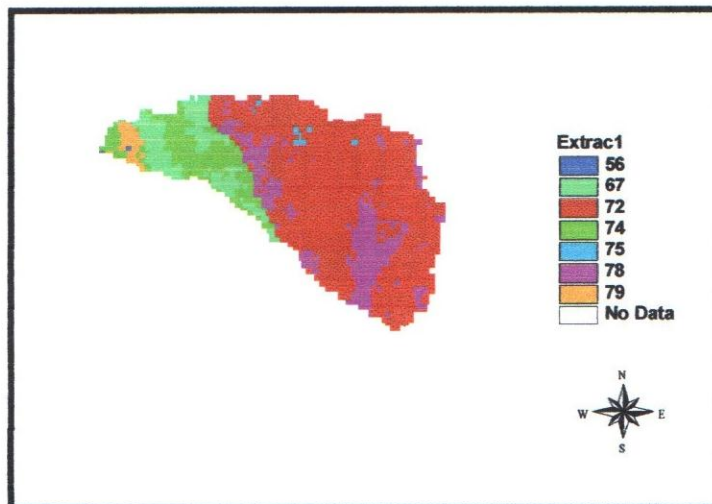
Figure 4.10: Runoff Curve Number for Tana Basin B

4.2.3 Physical Parameters of Tana Basin C

Below are table and figure indicating physical parameters for each sub-basin in Tana Basin C;

Table 4.3: Physical Parameters of Tana Basin C

Basin ID	Soil Water Holding Capacity (mm)	Soil Depth (cm)	Texture	Area (km^2)	Hill Slope	Runoff Curve Number
15	154.079	138.985	Loam	512.4	0.1262	64.5
13	102.063	114.719	Loam	1789.2	0.1421	75.2
11	109.379	119.177	Loam	1150.1	0.2099	75.6
9	111.379	120.387	Loam	61.6	0.5635	75.2
3	115.052	122.611	Loam	867.8	0.2366	75
2	119	125	Loam	134.4	0.2011	74.3
5	119	125	Loam	100.6	0.3143	77.7
6	108.911	118.893	Loam	1458.5	0.38	76.3
1	111.186	120.27	Loam	1208.6	0.3698	75.3
4	117.227	123.927	Loam	1159.9	0.4125	74.8
7	108.196	118.46	Loam	628.7	0.4949	75.6
14	100	113.5	Loam	477.2	0.1479	74.8
8	114.055	122.007	Loam	474.8	0.2923	77.6
10	118.477	124.683	Loam	467.8	0.3252	77.9
12	100	113.5	Loam	426.8	0.1938	75.1

Figure 4.11 shows the general elevation of Tana Basin C. Highest areas for the sub-basins were upper part and the lowest towards the outlet of the basin. All individual sub-basin inter-flow and surface run-off flow ended up in the Tana River.
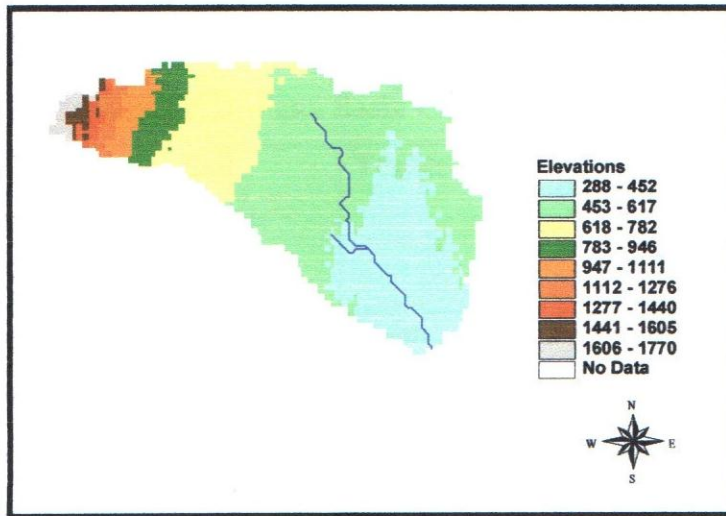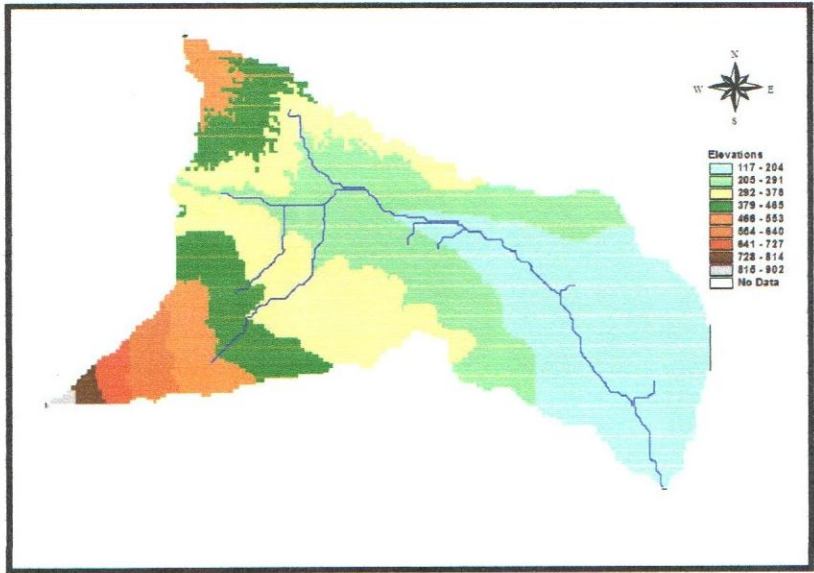
Figure 4.11: Elevation Tana Basin C (in meters)

Figure 4.12 shows the runoff curve number for Tana Basin C. Highest runoff curve number for the sub-basins was 77.9 and the lowest 64.5 along the Tana River. The sub-basins have very close runoff number curve (exccept for *sub-basin 15* with 64.5) due to the fact that the soil group, land use and hydrological condtions were almost the same for all of them.
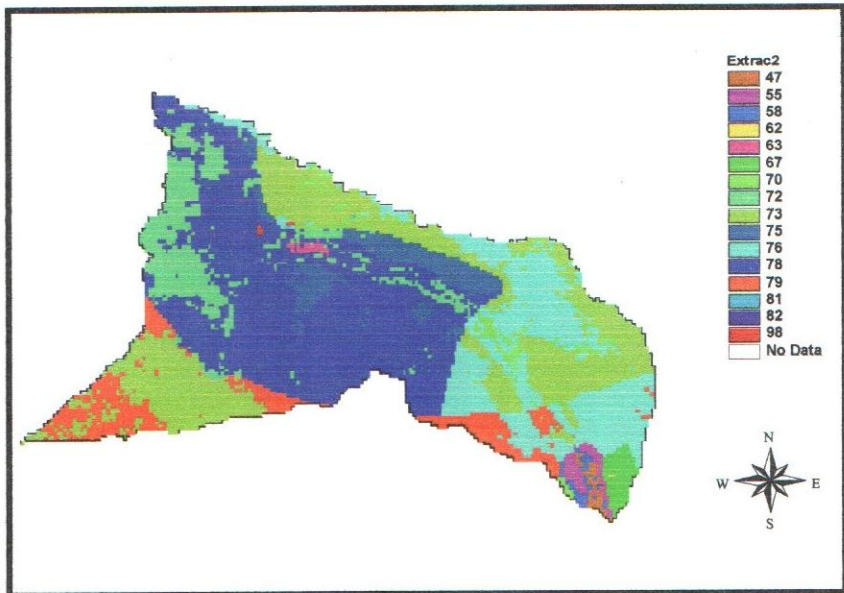
Figure 4.12: Runoff Curve Number for Tana Basin C

Figure 4.13 shows the soil depth for Tana Basin C. Highest soil depth for the sub-basins was 138.99 cm and the lowest 113.5 cm along the Tana River.
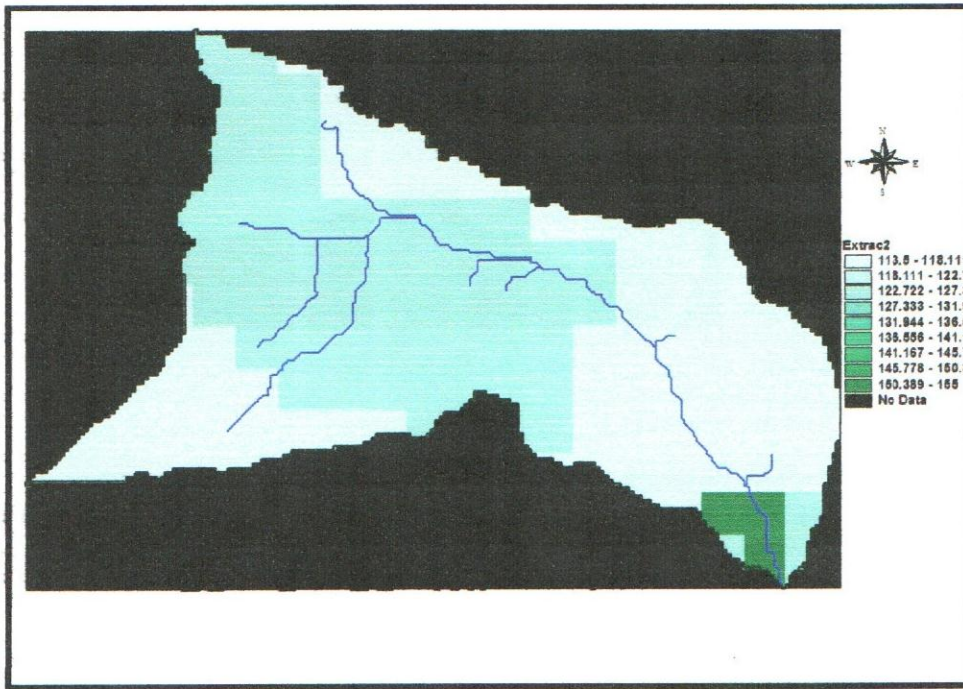
Figure 4.13: Soil Depth for Tana Basin C (in centimetres)

Figure 4.14 shows the soil water holding capacity for Tana Basin C. Highest soil water holding capacity for the sub-basins was 154.08 mm and the lowest 100 mm along the Tana River. The realtionship of runoff curve number, soil depth and soil water holding capacity for each individaul sub-basin were close.
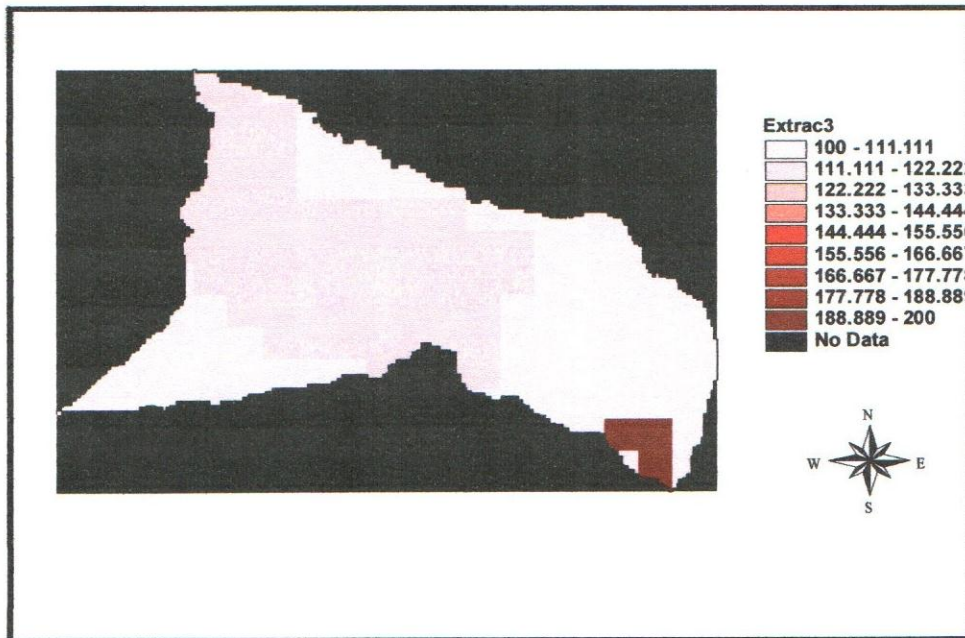
Figure 4.14: Soil Water Holding Capacity for Tana Basin C (in millimetre)

4.3   Rain Data

Meru station is the Middle Tana Basin (referred to as Tana Basin A in this study). The daily observed rainfall data for Meru Meteorological Station was used is this study. Tana Basin A has 11 sub-basins. Both daily observed ground and satellite rainfall estimate (RFE) data of Meru station (a sub-basin number 8 in Tana Basin A) for 1995 – 2006 were analyzed on annual basis.

The data was inserted in excel sheet and scattered point type of graph selected. Linear trend line was selected in the determination of the correlation of the two sets of data. A correlation (r^2) of was 0.8191 obtained. Figure 4.15 shows the correlation between daily observed ground and satellite rainfall for Meru station.
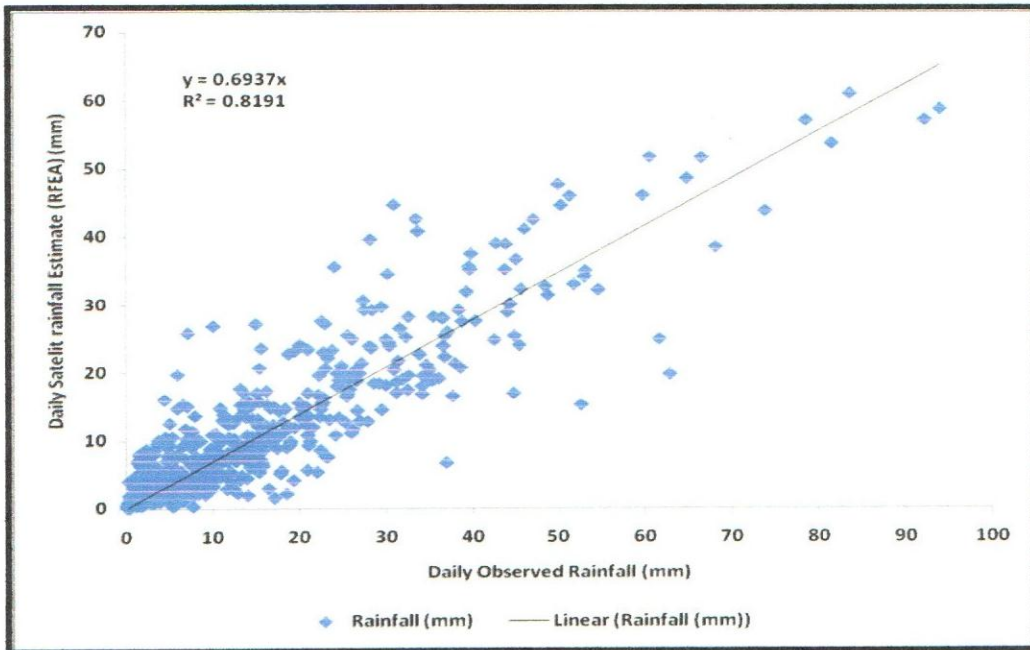
Figure: 4.15 Correlations between daily observed rainfall and Satellite RFE for Meru Station (1995 -2006)

Also a correlation of Meru sub-station's annual RFE against all other 10 sub-basin in the same Tana Basin A was determined. A relationship was also determined between Meru sub-basin and 10 other sub-basins in the same basin based on satellite RFE. These inter sub-basins relationship of Satellite RFE was used in estimating ground rainfall for all other sub-basins without meteorological station in the same basin. Meru station's ground rainfall (for sub basin 8) and the estimated other sub-basin's ground rainfall were used in both calibration and validation of the model.

Table 4.4 shows the correlation between daily Satellite Rainfall Estimate (RFE) for Meru (Sub-basin 8) and other Sub-basins in the same Tana Basin A for rainfall data of 1995-2006.

Table 4.4: Correlation between daily Satellite Rainfall Estimate (RFE) for Meru (Sub-basin 8) and other Sub-basins in Tana Basin A (1995-2006)

Sub-Basin ID	Correlation with basin 8
3	0.8611
2	0.9122
1	0.8839
4	0.8381
5	0.879
6	0.7567
7	0.883
10	0.8398
9	0.8617
11	0.8512

Garissa station is the Lower Tana Basin (referred to as Tana Basin C in this study). By the same method explained above a correlation (r^2) of 0.8186 was also determined for Garissa sub-basin by the use of annual daily observed ground and satellite rainfall estimate (RFE) for 1995 – 2006.

Figure 4.16 shows the correlation between daily observed ground and satellite rainfall for Meru station;
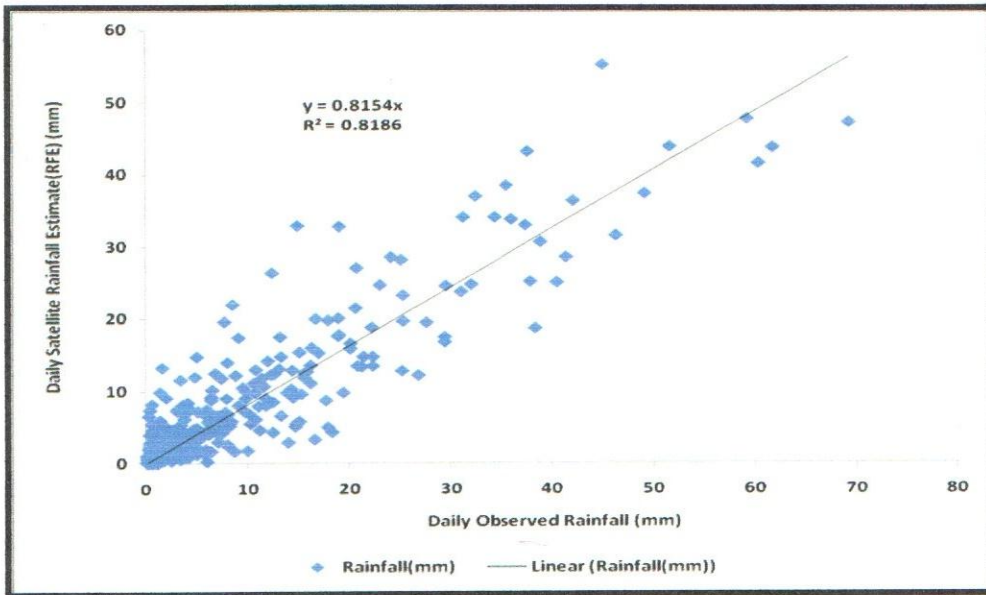
Figure 4.16: Correlations between daily observed rainfall and Satellite RFE for Garissa Station (1995 -2006)

Table 4.5: Correlation of daily Satellite Rainfall Estimate (RFE) for Garissa (Sub-basin 13) and other Sub-basins in Tana Basin C (1995-2006)

Sub-Basin ID	Correlation (r^2) with Sub-basin 13
15	0.736
11	0.852
9	0.7442
3	0.832
2	0.7818
5	0.7242
4	0.693
6	0.7287
7	0.6578
8	0.8333
10	0.7111
1	0.682
14	0.5138
12	0.8243

4.4   Parameter Sensitivity Analysis

The sensitivity analysis was done to determine physical parameters which were to be used for calibration and their feasible ranges. Soil depth, soil water holding capacity, pan coefficient for Evapo-transpiration loss (PET) correction and runoff curve number were found to be the most sensitive parameters with bigger impact on the model outputs due to changes in the model inputs. One-at-a-time per parameter method was used, where the model was run manual each time with only one parameter changed (within a range) many times while all other parameters were held constant. The parameter which gave the highest values of correlation coefficients (R^2) between annual daily simulated and observed stream-flow was found to be Pan coefficient for Evapo-transpiration (PET) loss correction (with 15 % adjustment).

Table 4.6 shows the results of the correlation of observed and simulated flow after adjustment of the soil depth by 30 cm. Three trials were done.

Table 4.6: Soil Depth

Parameter	Depth (cm)	Correlation (R^2) Observed/Simulated flow
Soil Depth	90	0.604
	120	0.5624
	150	0.4796

Table 4.7 shows the results of the correlation of observed and simulated flow after adjustment of the soil water holding capacity by 30 mm. Three trials were done.

Table 4.7: Soil Water Holding Capacity

Parameter	Depth (mm)	Correlation (R^2) Observed/Simulated flow
Soil Water Holding Capacity	90	0.5442
	120	0.5573
	150	0.5542

Table 4.8 shows the results of the correlation of observed and simulated flow after adjustment of the Pan Coefficient for Evapo-transpiration loss (PET) correction. Three trials were done.

Table 4.8: Pan Coefficient for Evapo-transpiration loss (PET) correction

Parameter	% Adjustment (reduced)	Correlation (R^2) Observed/Simulated flow
Pan coefficient for Evapo-transpiration loss correction	10	0.7948
	15	0.8055
	20	0.6419

Table 4.9 shows the results of the correlation of observed and simulated flow after adjustment of the Pan Coefficient for Evapo-transpiration loss (PET) correction. Three trials were done.

Table 4.9: Runoff Curve Numbers

Parameter	Depth (mm)	Correlation (R^2) Observed/Simulated flow
Runoff Curve Numbers	98	0.5955
	80	0.5955
	60	0.5955

4.5 Model Calibration and Validation

The model was calibrated in Meru sub-basin in the Tana Basin A (Middle Tana River basin). Kazita (F19) station's daily observed ground data of 1980 to 1982 was used because there were floods during these period and missing data were few. Pan coefficient for Evapo-transpiration loss (PET) correction (most sensitive parameter) was adjusted (reduced) by 15 % in the model's basin text file. The model was calibrated manually as there was no algorithm for automatic calibration. The model simulated daily stream flow

from the input files. The rainfall (precipitation) was converted into evapotranspiration, surface run-off, interflow, base-flow and ground water components at the end of each time step. The observed ground daily stream-flow data of Kazita (F19) station for 1980 to 1982 was separated into daily base-flow and flow caused by surface run-off from rainfall effects. This separation of base-flow was done by the use of semi-log graph paper. The annual daily base flow data were converted into natural $\log_e$ (ln) and used against time (1 year). The correlation of annual daily simulated and observed stream-flow data of Kazita (F19) for the 1980 to 1982 was tested after calibration for all flows (low and high flows). The correlation (r^2) of observed and simulated flow after calibration of the model using Kazita Station (4F19) for daily stream flow data of 1980-82 was 0.8296. This Correlation is shown on Figure 4.17 below;
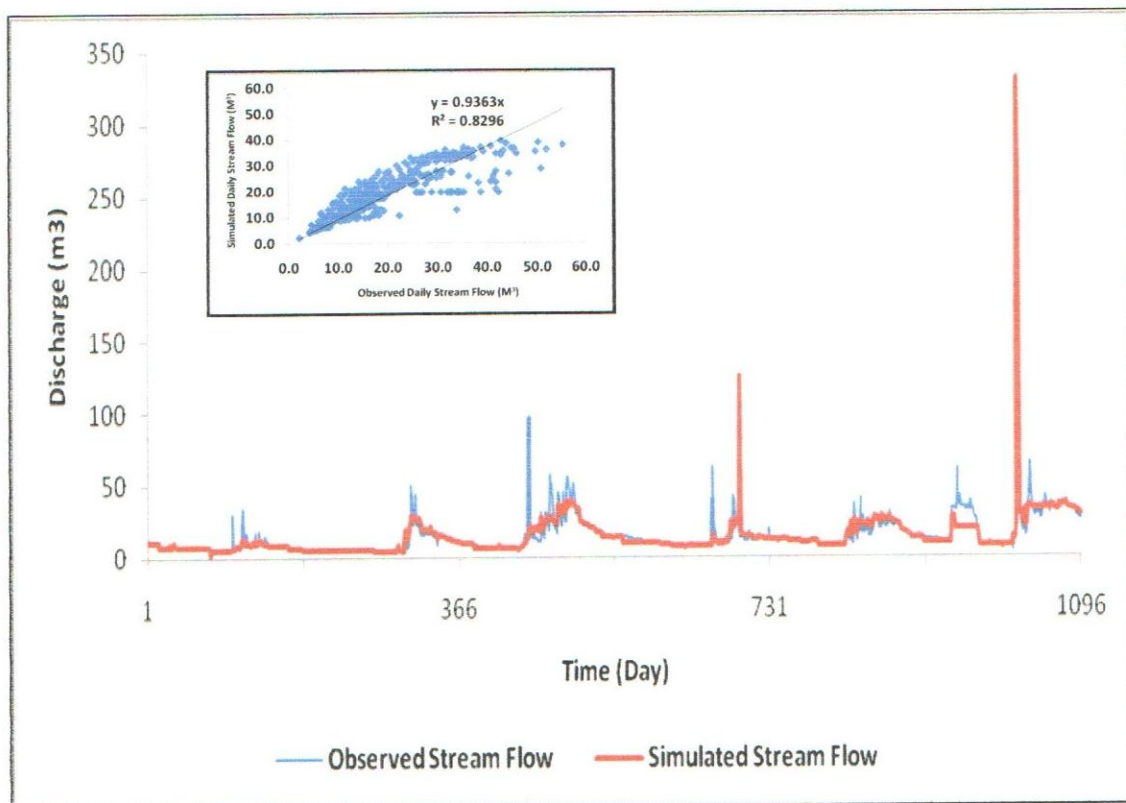

Figure 4.17: Correlation (r^2) of observed and simulated flow after calibration of the model using Kazita Station (4F19) for daily stream flow data of 1980-1982

After the model was calibrated with plausible parameter values, the model was validated using the same adjusted parameter in calibration. Observed daily streamflow data of Kazita (4F19) and Garissa (4G1) ground gauging station for 1986 to 1988 was separated in the same process as stated above into daily base-flow and flow caused by surface run-off from rainfall effects. In the validation process a correlation was determined between annual daily simulated and observed stream-flow for each of these two stations for 1986-88 period. The correlation (r^2) after validation of the model at Kazita Gauging station (4F19) is 0.8064 as shown in Figure 4.18.
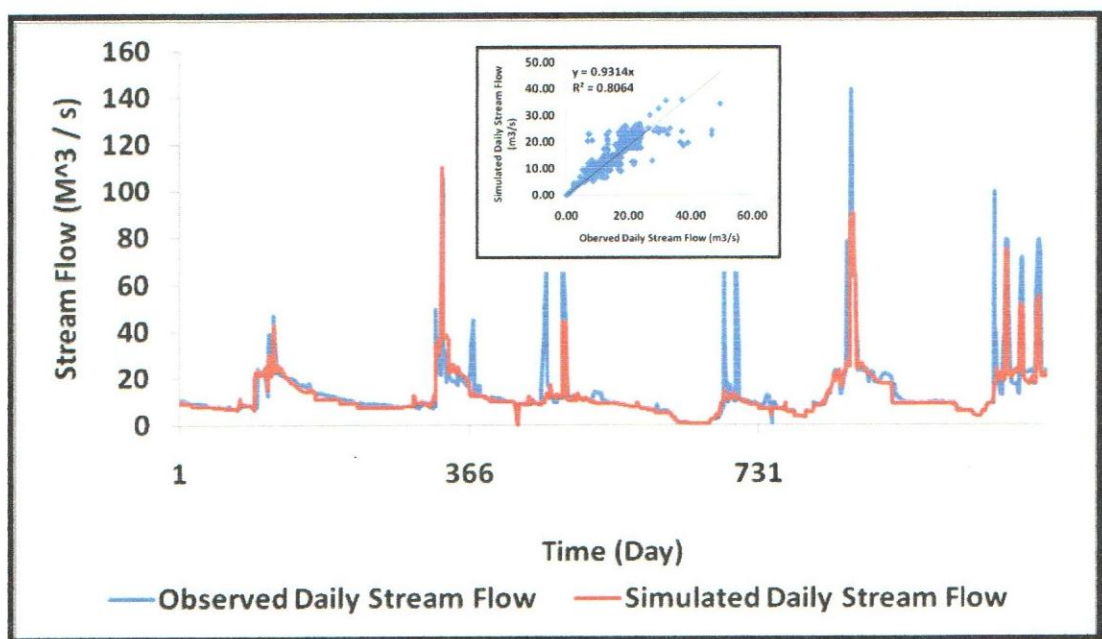

Figure 4.18: Correlation (r^2) of observed and simulated flow after validation of the model using Kazita Station (4F19) for daily stream flow data of 1986-88

The correlation (r^2) after validation of the model at Garissa Gauging station (4G1) is 0.7389 as shown in Figure 4.19.
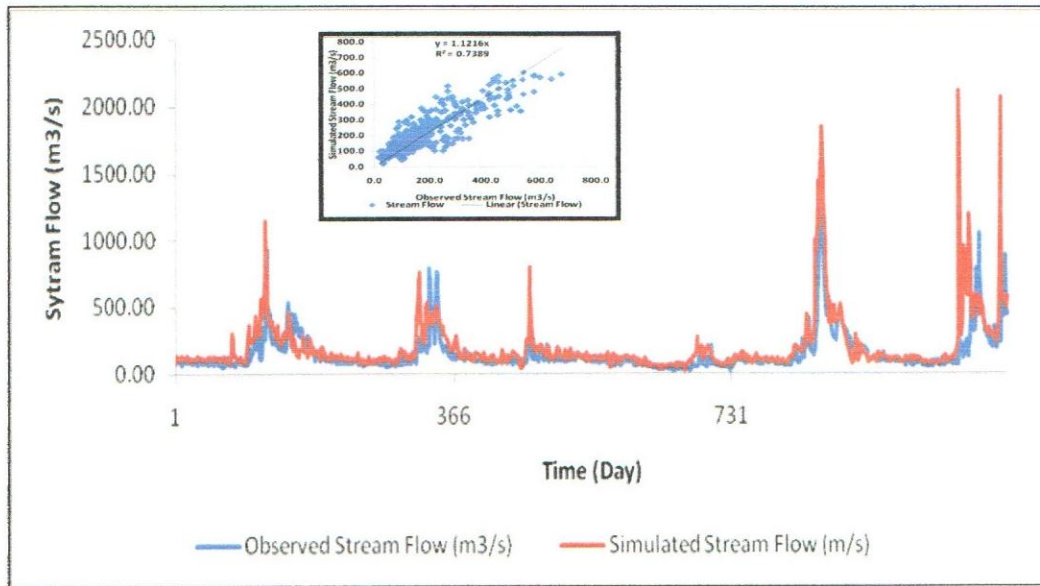
Figure 4.19: Correlation (r^2) of observed and simulated flow after validation of the model using Garissa Station (4G1) for daily stream flow data of 1986-88

After calibration and validation it can be seen that the model simulates daily stream based on water balance principle of separating the only input rainfall (precipitation) into evapotranspiration, surface run-off, inter-flow, base-flow and ground water components at the end of each time step. The days with no rainfall the surface runoff component that contributes to simulated stream flow is zero depending on the sub-basin's response or time of concentration. At such times the river carries only base-flow.

4.6 Stream Flow Forecasting

The model can be used for short period/lead time of 1 to 3 days forecasting of flood between stream gauging stations. The flood flow data of one day before the peak flood was put into steady gradually varied channel geometry in order to forecast flood level at points down stream. The model was run twice independently. As an example on Table 4.11, for the first time the data used in running the model was from day 1 to day 122 and second round was from day 1 to day 119. At the end each of the runs the model generated three days of forecasting flow. Day 120 to day 122 data gives the actual flow for first run and forecasted flow for the second run. Below are tables that compare the simulated and the forecast flood by the model for the same period along the Tana River in Tana Basin A. Sub-basin 3 was used in this comparison with data of 1982 and 1988.

67

Below are tables showing the relationship of the simulated and forecast for the three days;

Table 4.10: Flood Flow Forecasting in Sub-Basin 3 of Tana Basin A

Day (1982)	Actual simulated daily stream (m³/s)	Forecasted Stream Flow (m³/s)	% Deviation
289	148.47		
290	1010.1		
291	2232.94		
292	2433.98	2389.52	1.83
293	2053.07	1784.77	13.06
294	1681.27	1189.76	29.23

Table 4.11: Flood Flow Forecasting in Sub-Basin 3 of Tana Basin A

Day (1988)	Actual simulated daily stream (m³/s)	Forecasted Stream Flow (m³/s)	% Deviation
127	108.98		
128	226.2		
129	238.38		
130	296.15		
131	461.34	461.34	0
132	408.89	408.9	- 0.002
133	275.03	275.03	0

Table 4.12: Flood Flow Forecasting in Sub-Basin 3 of Tana Basin A

Day (1988)	Actual simulated daily stream (m³/s)	Forecasted Stream Flow (m³/s)	% Deviation
116	872.28		
117	739.48		
118	614.89		
119	792.38		
120	835.42	835.89	- 0.06
121	617.55	619	- 0.23
122	416.77	419.46	- 0.64

There is little deviation in the comparison of actual simulated an forecasted stream flow The results in above tables 4.10-4.12 indicates that USGS Stream Flow Model can used for peak flood flow forecasting.

4.7 Updating Bank-full and Flow Statistics (Post-Processing)

The model generated the final updated output riverstats.txt file with statistical estimate of carrying capacity (maximum) of channels or streams in every sub-basin. Any flow stream or river flow above maximum or bank-full is assumed to be flood flow in the lower Tana flood plains. In this case the model determined bank-full flows at the three proposed potential diversion sites and Garissa river gauging station. These bank-full flows are shown on Table 4.13 below;

Table 4.13: Bank-Full or Maximum Flows

Site	Maximum Flows (m³/s)
Diversion 1 (proposed)	1194.1
Diversion 2 (proposed)	1193.6
Diversion 3 (proposed)	1183.1
Garissa Station (4G1)	1141.2

The model determines the bank-full flow at Garissa Station (4G1) as 1141.2 m^3/s. According to Dwars Heederik en Vertey (DHV, 1986) the actual observed cross-section dimension gives the bottom width as 140 m, top width as 156 m, depth as 4.5 m, river bed slope as 0.034 % and side slopes as 1.5. After applying continuity equation as of 1099.22 m^3/s was determined. The model's bank-full flow of 1141.2 m^3/s at Garissa Station (4G1) is close to the actual of 1099.22 m^3/s. Therefore, we estimate the bank-full at three proposed diversion sites as shown in Table 4.10. Any flow above this figure of bank-full is flood water flow that will be diverted through the three proposed diversions.

4.8   Proposed Diversion Sites

Three ideal points were identified by the use of sub-basin physical features generated by the model's terrain analysis function and contours from the topo-maps as possible potential sites for diversions. The possibility of water flowing through diversion channels between the two basins depended on the topographical difference between the proposed outlet from Tana River and inlet at Ewaso Ng'iro Basin. Contours assisted in determining the course for each diversion channel. The bed slopes of Lower Tana River according to Kenya Datum are shown below in Table 4.14;

Table 4.14: Bed slopes of Lower Tana River

Distance (Km)	Elevation Difference (m)	Sloped	Remarks
0 – 100	7	$7 * 10^{-5}$	Starts at Indian Ocean
100 – 200	21	$2.1 * 10^{-4}$	
200 – 300	28	$2.8 * 10^{-4}$	
300 – 400	38	$3.8 * 10^{-4}$	Bura at 371 km
400 – 500	33	$3.3 * 10^{-4}$	Nanigi at 420 km
500 – 600	50	$5 * 10^{-4}$	Garissa at 509 km
600 – 630	17	$5.67 * 10^{-4}$	Mbalambala at 622 km

Source of data: Tana River Morphology Study (DHV, 1986)

Assume the bed slopes of the proposed diversion channels are between $7 * 10^{-5}$ and $5.67 * 10^{-4}$. Then the three proposed channels will be able to connect the Tana and Ewaso Ng'iro Basin basins. The three points were identified from the topo-maps and supported by complete terrain analysis (USGS Streamflow Model) as possible sites for diversion of some part of the flood water are shown in Table 4-14 together with their position and altitude;

Table 4.15 : Proposed Diversion Sites

Name	Bearing of Proposed Diversion Sites	Altitude	Remarks
Diversion 1	S 0^0 04' 29.6" E $38^0$24' 4.7"	360 meters	At Adam's Fall
Diversion 2	S 0^0 02' 40" E 38^0 40' 0"	294 meters	About 6 km upstream of Kora Rapids
Diversion 3	S 0^0 05' 00" E 38^0 48' 00"	240 meters	At Kora Fall

Terrain analysis through the guide of the contour maps assisted in the determination of the positions of the three proposed diversion sites and also was used in estimation of the daily surface runoff that each contributed to their individual daily flow. Diversions 1 and 2 are in Tana Basin A and diversion 3 is in Tana Basin B.

Diversion 1: It's at Adam's fall next to the bridge, in Meru Game Reserve. It's ideal site for diversion as there are good bed rocks. The disadvantage is that, the contour 360 crosses the Bisaanadi River (Tributary of Tana) at some point. It's also too long (it stretches about 90 km to the ridge that divides the Tana and Ewaso Ng'iro basins). It commands a bigger area. See Appendix D1 for a map showing the position of proposed Diversion 1.

Diversion 2: It's about 25 km upstream of Mbalambala water supply in-take. It's the most ideal site. The length of the proposed channel from this point to the ridge that divides the Tana and Ewaso Ng'iro Basins is about 65 km. It can drain to part of western

71

lagga and eastern lagga of Ewaso Ng'iro basin. See Appendix D2 for a map showing the position of proposed Diversion 2.

Diversion 3: This point is about 8 km upstream of Mbalambala water supply in-take. It's the only in-take in the North Eastern Province. It will be the longest ((it stretches about over 120 km to the ridge that divides the Tana and Ewaso Ng'iro Basins). It will deliver its water after Garissa town. It can be used by farmers as gravity intake to their farms (from Mbalambala to downstream of Garissa). See Appendix D2 for a map showing the position of proposed Diversion 3.

4.9   Estimated Flood Magnitude at Proposed Diversion Sites

Magnitude of flood flow at these three ungauged proposed potential diversion sites were determined by use of daily stream flow of Grand Fall Station (F13) as an addition to the already validated daily stream flow simulated by the model for the Tana Basin A and Tana Basin B. The position of Grand Fall Station (F13) is the most upstream starting point of Tana Basin A. The data for years 1986 – 1998 was used in the generation of these estimated daily stream flow for the three proposed potential site. The model is able to simulated estimated daily stream flows at the three (ungauged) proposed diversion sites. It is assumed that the amount of water abstracted along the river channel is negligible if compared to flood flows. The positions of these ungauged sites are provided in the Appendix (Figures A1 to A3).

CHAPTER 5

CONCLUSION AND RECOMMENDATION

5.1   Conclusion

The study was carried out with the aim to evaluate the magnitude of flood flow in Lower Tana to facilitate mitigation measure and economic use of the flood. This was achieved through the use of USGS Stream flow model for simulation of flood flow and determination of potential flood diversion sites. Geo-information, meteorological and hydrological data were collected for the three basins along Tana River. Raw data were checked for missing ones and out-liars eliminated. The model simulated daily stream flow along the middle and lower Tana River for 1980–82 (during calibration) and 1986–88 (during validation). The correlation of daily simulated and observed stream-flow data of Kazita station (F19) for the 1980 to 1982 data was tested after calibration for all flows (low and high flows). The correlation (r^2) of observed and simulated flow after calibration of the model using Kazita Station (4F19) for daily stream flow data of 1980-82 was 0.8296. The model was validated using the same adjusted parameter in calibration. Daily simulated and observed stream-flow data 1986-88 of Kazita station (F19) Observed daily stream-flow data of Kazita (F19) and Garissa was used for validation of the model. The correlation (r^2) after validation of the model at Kazita station (4F19) was 0.8064 and Garissa station was 0.7389. Therefore, USGS Stream flow model can be used for simulation of flood flows.

Through this simulation process the estimation for the magnitude of flood flow at the three proposed potential sites were determined. Three ideal points were identified for possible inter-basin water transfer by the use of sub-basin physical features generated by the model's terrain analysis function and contours from the topo-maps as possible potential sites for diversions. These were Diversion 1 (S 0^0 04' 29.6'', E $38^0$24' 4.7''), Diversion 2 (S 0^0 02' 40'', E 38^0 40' 0'') and Diversion 3 (S 0^0 05' 00'', E 38^0 48' 00''). The estimated magnitude of flood flow at these three un-gauged proposed potential diversion sites were determined by use of already validated daily stream flow simulated

by the model for the Tana Basin A and Tana Basin B. The model determined the bank-full or maximum flows at the three proposed potential diversion sites and Garissa river gauging station. The model's bank-full flow of 1141.2 m^3/s at Garissa Station (4G1) is close to the actual (at the same site) of 1099.22 m^3/s. Any flow above the figure of bank-full or maximum is flood water flow that could be diverted through the three proposed diversions.

5.2   Recommendation

Frequency analysis should be done to determine design floods of certain magnitudes and their return periods for each of the three proposed diversion sites. This study will assist in the designs of the flood water diversion channels.

REFERENCES

Abuodha, P. and Omenge, J., 2004. Modern Mega Flooding in Kenya especially Budalangi Division and Tana River Districts. Proceedings of Workshop on "Mega-floods: How to identify mega-floods in palaeorecords", Bobole – Mozambique

Agwata, J. F., 2006. Resource Potential of the Tana Basin with Particular Focus on the Bwathonaro Watershed, Kenya

Anderson, D. J., 2000. GIS-based hydrologic and hydraulic modeling for floodplain delineation at highway river crossings. M.Sc. Thesis. University of Texas at Austin, United State of America.

Artan, G. A., Kiesler, J.L., Asante, K. O. and Verdin, J., 2001. Use and Description of the Famine Early Warning System Flood Model.

Asante, K. O., Artan, G. A., Pervez, S., Bandaragoda, C. and Verdin, J. P., 2009. Technical Manual for the Geospatial Stream Flow Model (GeoSFM). U.S. Geological Survey, Reston, Virginia.

Biswas, A. K., 1983. Long-distance water transfer: Problems and Prospects. United Nations University, Water Resources Series, Volume 3.

Choudhury, P., Narulkar, S.M. and Shrivastava, R.K., 2002. Flood routing in river networks using equivalent muskingum inflow. J. Hydrol. 7(6): 413 – 419.

Chow, V.T., Maidment, D.R. and Mays, L.W., 1988. Applied Hydrology. International edition. McGraw-Hill Book Company New York.

Deputy Prime Minister and Minister for Finance, 2009. Flood Disaster Management by adoption to climate change in Nyando River Basin. Speech of Deputy Prime Minister

and Minister for Finance, Kenya.

DHV, 1986. Tana River Morphology Studies, Kenya.

Duivendijk, J. V., 1999. Thematic Review : Assessment of Flood Management Option. World Commission on Dam.

Famba, S.I., 2004. The 2000 flood in the lower Limpopo River basin. Proceedings of Workshop on "Mega-floods: How to identify mega-floods in palaeorecords", Bobole, Mozambique.

Fread, D.L., 1993. Flow Routing. In: Handbook of Hydrology. McGraw-Hill, Inc. New York.

Hirji, R., Partoni, F. M. and Rubin, D., 1996. Proceedings of the Seminar on Integrated Water Resources Management in Kenya.

Hudgens, B. T. and Maidment, D. R., 1999. Geospatial Data in Water Availability Modeling. Center for Research in Water Resources, Bureau of Engineering Research, University of Texas, Austin, USA.

Integrated Water Resources Management, 2007. Economic Aspects of Integrated Flood Management. WMO-No.1010.

Jacobs, J., Angerer, J. and Vitale, J., 2004. Exploring the Potential Impact of Reforestation on the Hydrology of the Upper Tana River Catchment and the Masinga Dam, Kenya.

Linsley, R.K. and Franzini, J.B., 1979. Water Resources Engineering. Third edition. McGraw-Hill, New York.

Linsley, R.K., Kohler, M.A. and Paulhus, J.H., 1992. Hydrology for Engineers. Third edition. McGraw-Hill international Book Company, Singapore.

Maingi, J.K. and Marsh, S.E., 2002. Quantifying hydrologic impacts following dam construction long the Tana River, Kenya. J. of Arid Environment 50:53-79.

Manuaela da G.M., 2004. Flood hazard assessment and zonation in the Lower Limpopo, Mozambique. M.Sc. Thesis, International Institute for Geo-information Science and Earth Observation Enschede, the Netherlands.

McCuen, R. H., Knight, Z and Cutter, A. G., 2006. Evaluation of the Nash–Sutcliffe Efficiency Index. J of hydrologic engineering 11: 597–602

Miller, W.A. and Cunge, K.A., 1975. Simplified equation of unsteady flow in open channels. Water Resources Publications 5: 183-257

Ministry of Water & Irrigation, 2006. The National Water Resources Management Strategy. First Draft.

Ministry of Water Development, 1992. The Study on the National Water Master Plan, Kenya.

Muthusi, F. M., 2004. Evaluation of the USGS Streamflow Model for Flood Simulation (Nyando Basin Case Study). M. Sc. Thesis. Jomo Kenyatta University of Agriculture and Technology, Kenya.

Mutua, B. M. and klik, A., 2007. Predicting daily streamflow in ungauged rural catchments: the case of Masinga catchment, Kenya. J. of hydrology sciences 52(2):292-304.

Mutua, B. M., Klik, A. and Loiskandl, W., 2005. Predicting Sediment Loading into Masinga Reservoir and its Storage Capacity Reduction. Paper No: II.09, International Symposium on Water Management and Hydraulic Engineering, Ottenstein, Austria.

Nash, J.E., and Sutcliffe, J.V., 1970. River flow forecasting through conceptual models. J. Hydrol. 10:282-290.

Northern Water Service Board, 2006. Proposed Flood Mitigation in Lower Tana, Kenya. Proceedings of Stakeholders Workshop on proposed Tana-Ewaso Ng'iro North inter-basin water transfer. Masinga Lodge, Kenya.

Omach, T. and Ti Le-Huu, T., 2003. Overview of the natural disaster and flood forecasting and warning systems in the Region. Proceedings of the Asia and the Pacific Regional Consultation workshop on preparation for early warning systems-II, Bandung, Indonesia.

Onyando, J. O., 2000. Rainfall-Runoff Model for Ungauged Catchments in Kenya. PHD Thesis, Ruhr University, Germany.

Onyando, J. O., Musila, F. and Awer, M, 2005. The use of GIS and Remote Sensing techniques to analyse water balance of Lake Bogoria under limited data conditions. J. of Civil Engineering 2(1):53–65.

Otieno, J.A., 2004. Scenario study for Flood Hazard Assessment in the lower Bicol Floodplain Philippine using A 2D Flood model. M.Sc. Thesis, International Institute for Geo-information Science and Earth Observation Enschede, the Netherlands.

Patil, S. R., 2008. Regionalization of an Event Based Nash Cascade Model for Flood Predictions in Ungauged Basins. PHD Thesis, Institute of Hydraulic Engineering, Universität Stuttgart, Germany.

Provincial Director of Agriculture and Livestock Extension NEP, 2003. Annual Report 2003- North Eastern Province, Kenya.

Provincial Director of Agriculture and Livestock Extension NEP, 2003. Flood Assessment Report-North Eastern Province, Kenya.

Provincial Planning Officer NEP, 2003. Proposed Investment Projects in North Eastern Province, Kenya.

Sharma, D. C. and Dubey, O. P. 2006. Terrain modeling in GIS for flood plain zoning. Irrigation Research Institute Roorkee, India.

Shaviraachin, T., 2005. Flood Simulation. A Case Study in The Lower Limpopo Valley, Mozambique, using the Sobek Flood Model. M.Sc. Thesis, International Institute for Geo-information Science and Earth Observation Enschede, the Netherlands.

Snead, D. B., 2000. Development and Application of Unsteady Flood Models using Geographic Information Systems. M. Sc. Thesis. University of Texas at Austin, USA.

Tokar, A. S. and Artan, G. A., 2006. Asia Flood Network: USAID/OFDA Flood Mitigation and preparedness program in Asia.

UNEP, 2002. Early Warning, Forecasting and Operational Flood Risk Monitoring in Asia (Bangladesh, China and India). Proceedings of the Project Workshop (GT/1010-00-04), Sioux Falls, SD, USA.

United Nation - World Water Development Report, 2006. 'Water: A shared responsibility'. Case study: Kenya National Water Development Report.

United State Army Corps of Engineers, 1998. HEC-1, Flood Hydrograph Package. User's Manual. Hydrologic Engineering Center, United State of America.

Wambua, S., 2003. Yatta Canal: The 'Nile' of Northern Machakos. Newsletter: A Water and Sanitation Resource Network (NETWAS).

Water Resources Management Authority, 2006. Buathonaro River Water Resources Users Association (BUAWRUA) Management. Induction Workshop, Kenya.

Wheater, H. S., 2004. Modeling Hydrological Processes in Arid and Semi Arid Areas.

World Meteorological Organization, 2004. Integrated flood management. Concept paper.

World Meteorological Organization, 2006. Environmental aspects of Integrated Flood Management, WMO-No. 1009.

World Meteorological Organization, 2006. Social aspects and stakeholder involvement in Integrated Flood Management, WMO-No. 1008.

World Meteorological Organization, 2008. Urban flood risk management. A tool for integrated flood management.
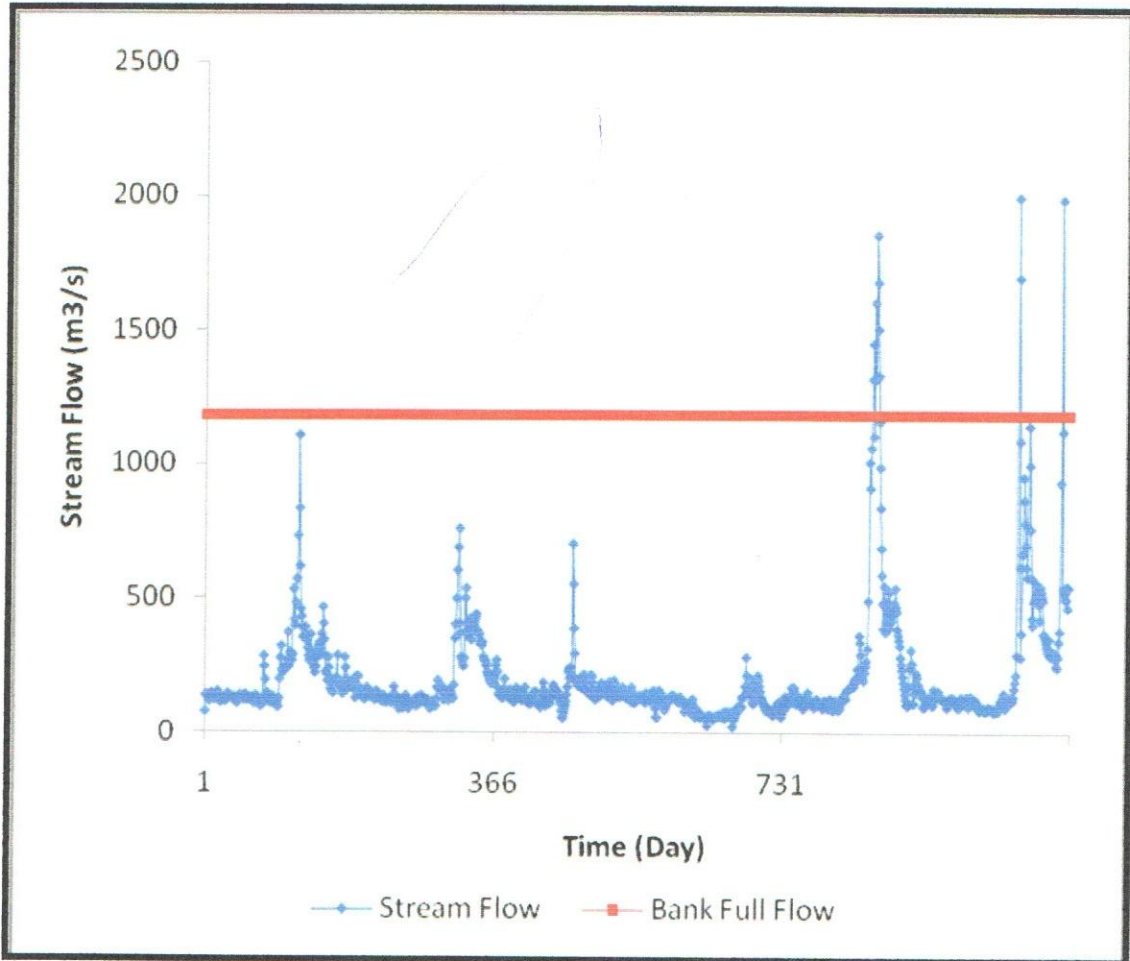
Yap, J. T. L., 2009. Traditional Flood Management Practices and Future Challenges, WMO, Jakarta, Indonesia.
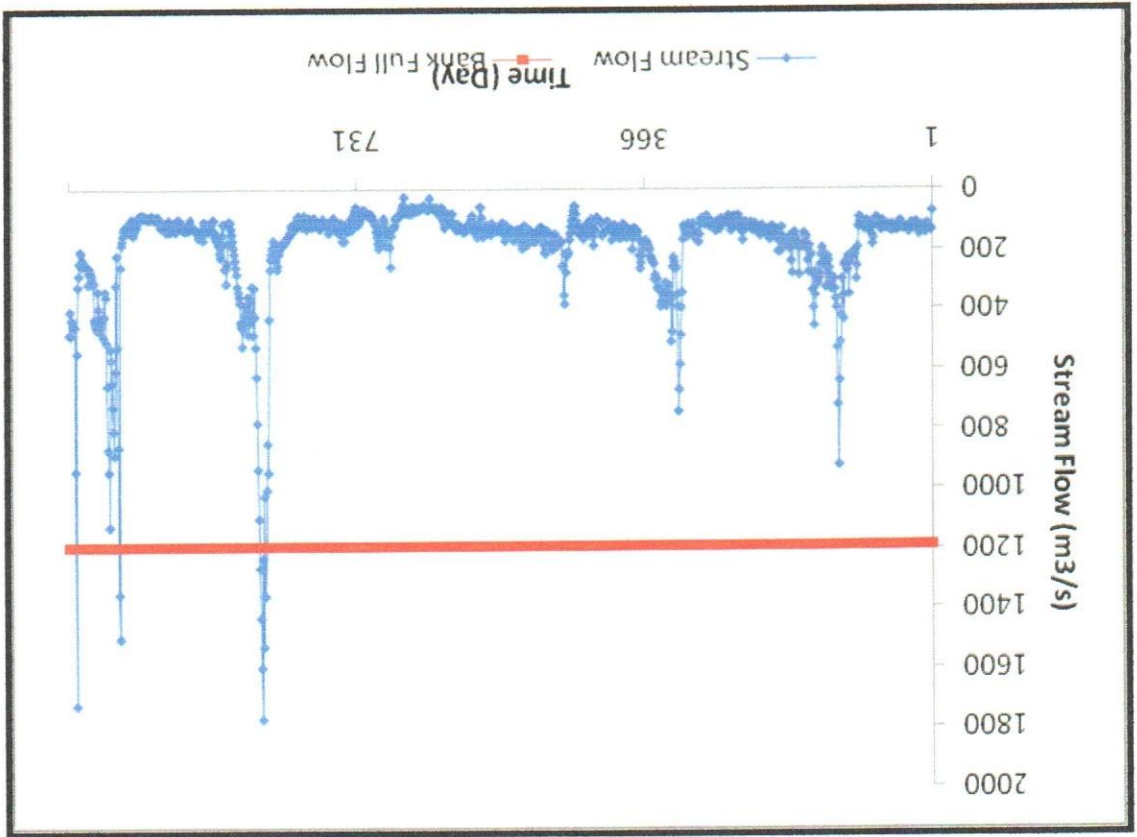
APPENDICES

APPENDIX A1: Simulated Daily Streamflow at proposed potential Diversion Site 1 (1986 – 1988)
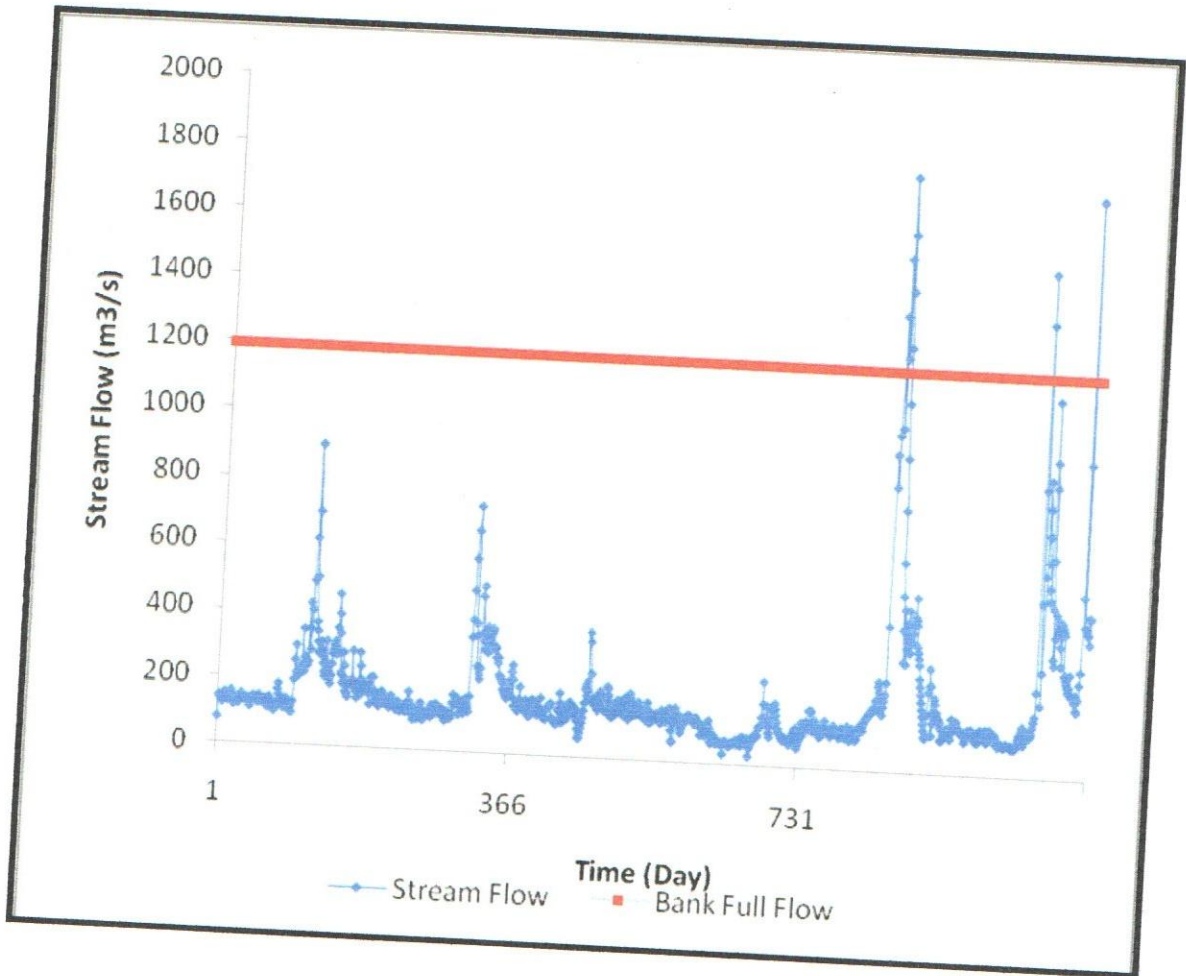
APPENDIX A2: Simulated Daily Streamflow at proposed potential Diversion Site 2 (1986 – 1988)

APPENDIX A3: Simulated Daily Streamflow at proposed potential Diversion Site 3
(1986 – 1988)

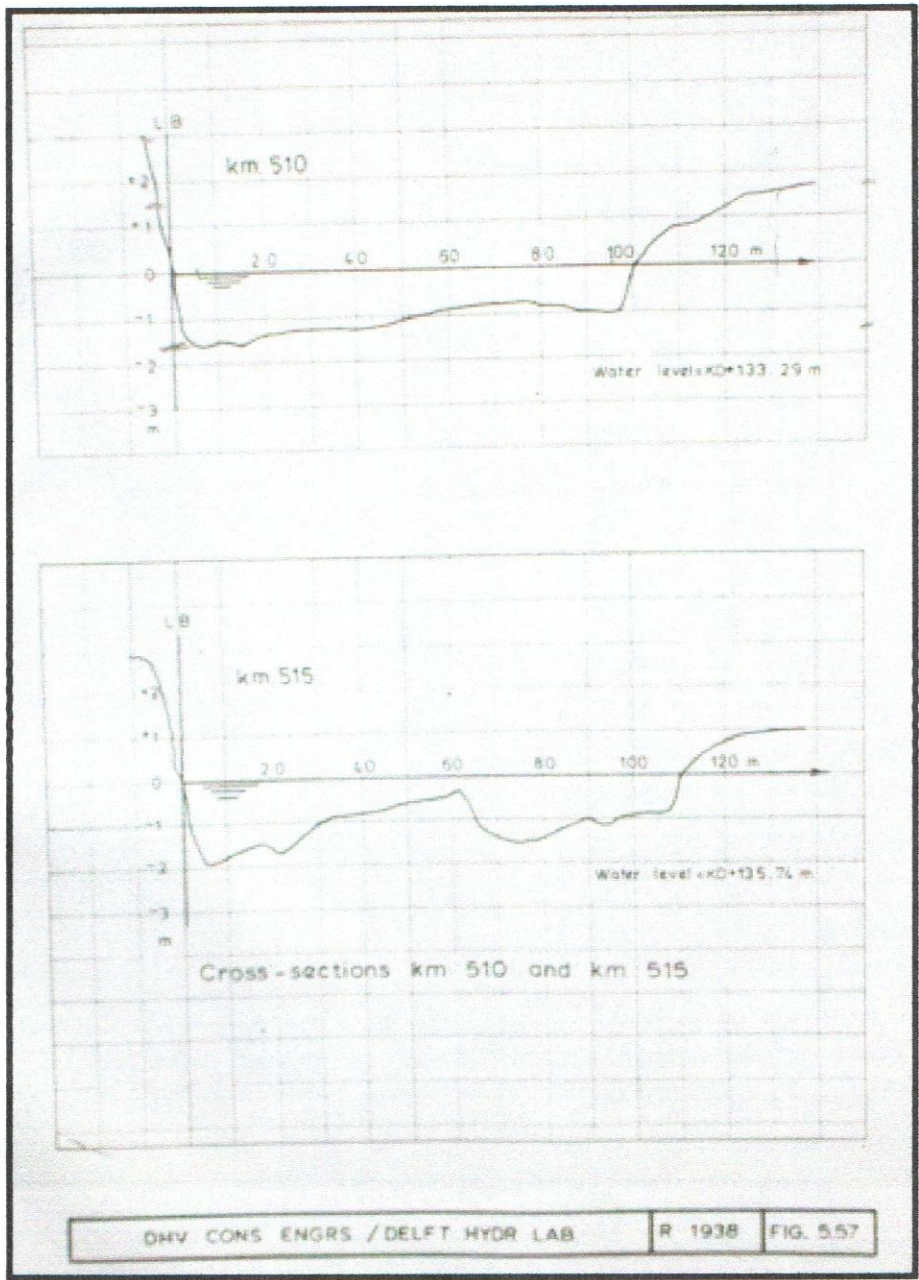**APPENDIX B1: Bura Irrigation Scheme (NIB) intake site along Tana River**

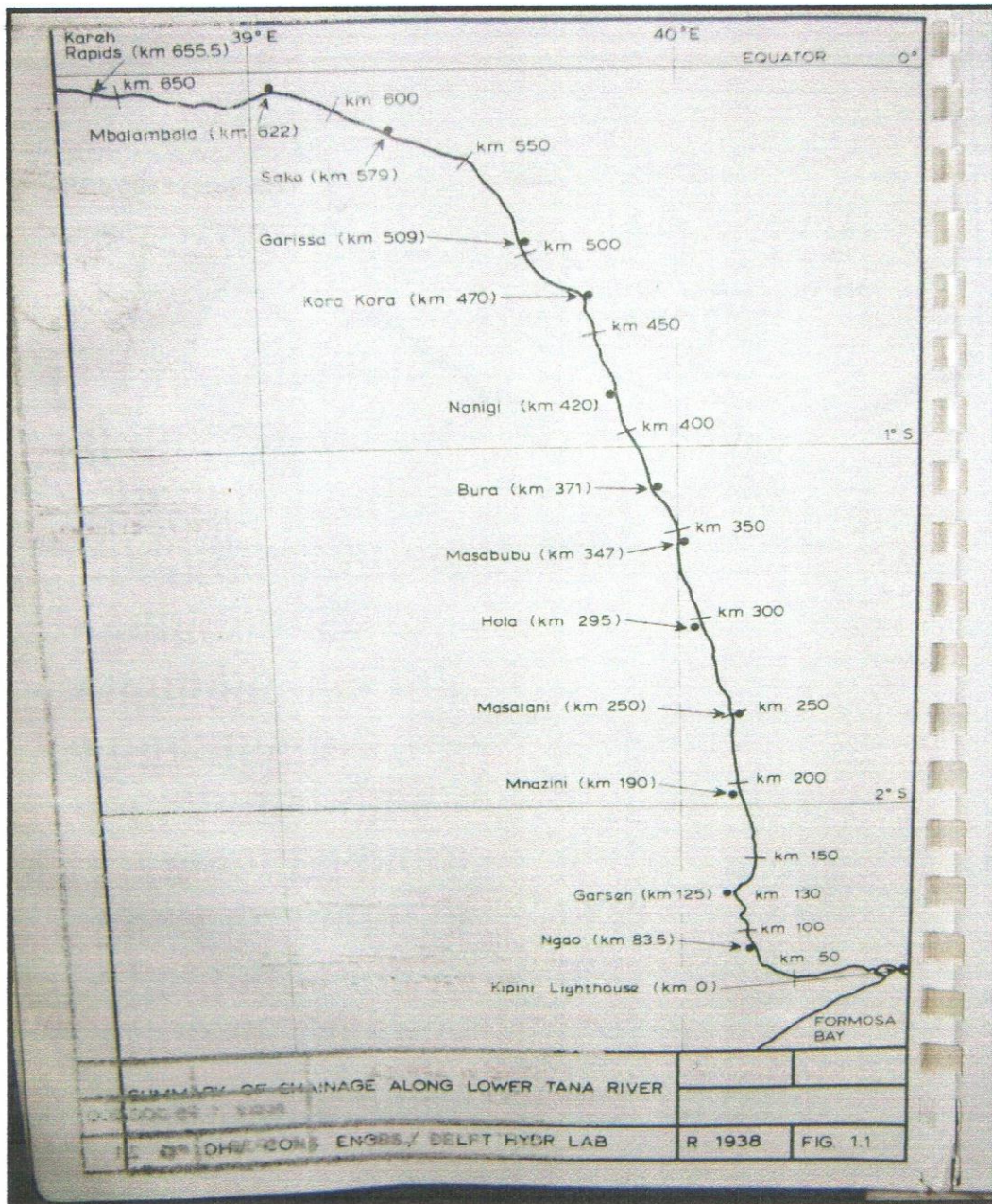**APPENDIX B2: Tana River near Garissa Gauging Station 4G1**

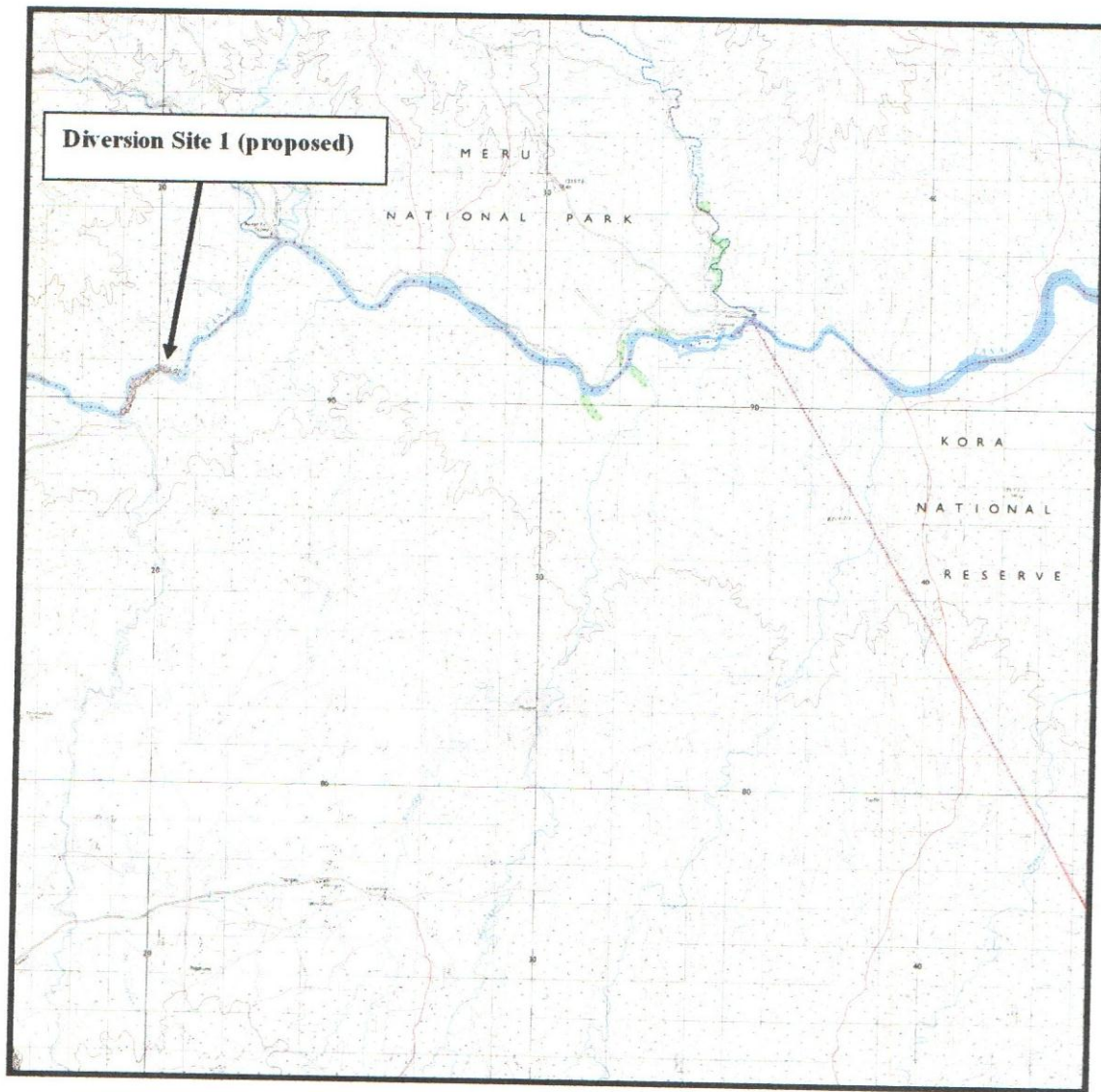**APPENDIX C1: Tana River's cross-section near Garissa Gauging Station (4G1) (Source: DHV, 1986)**
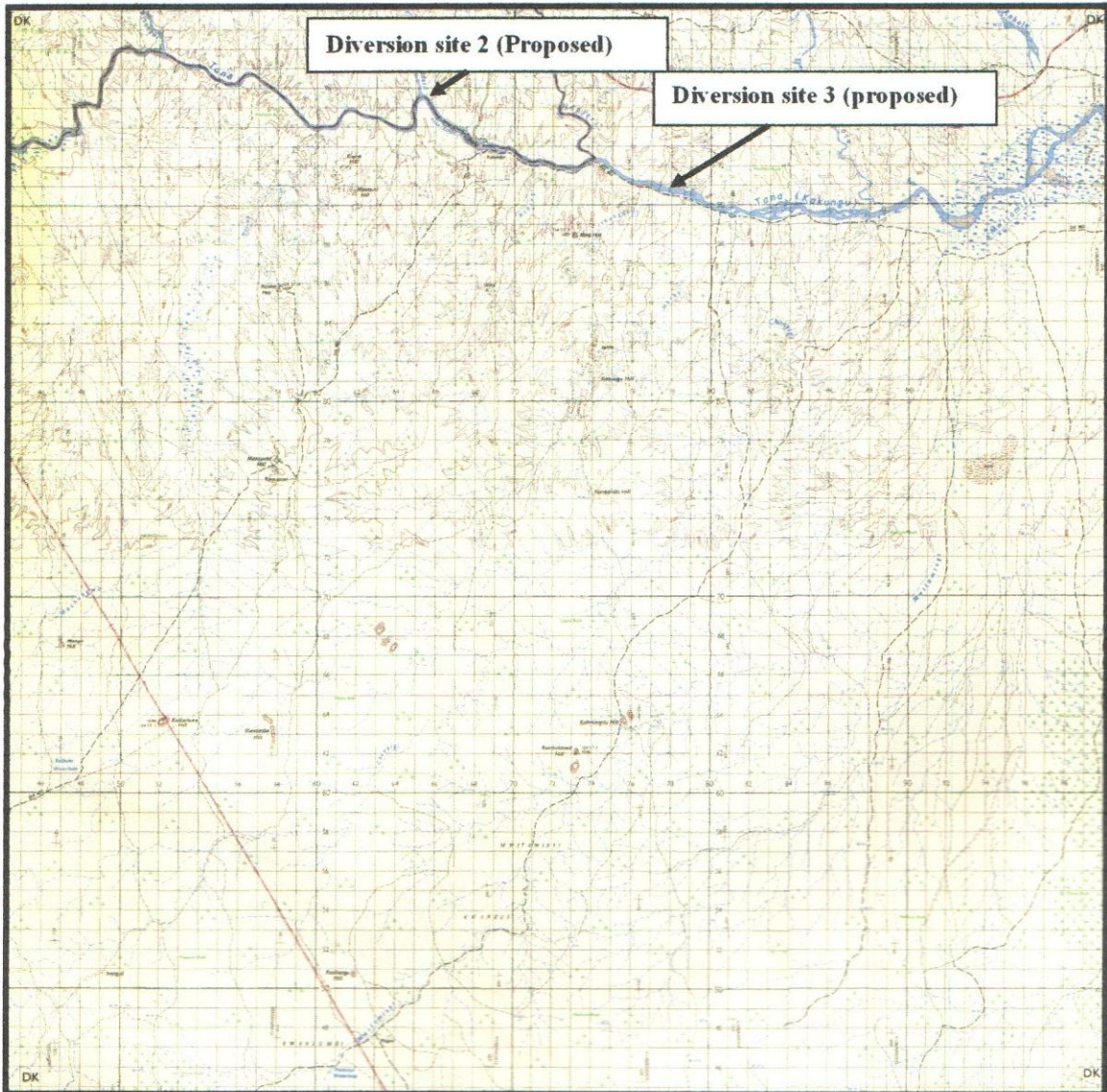

Cross-sections km 510 and km 515

APPENDIX C2: Chainage along Lower Tana River (Source: DHV, 1986)

APPENDIX D1: Site for Diversion 1 (proposed) along Tana River (Source: Survey of Kenya, Sheet 123-2)

APPENDIX D1: Site for Diversion 2 and 3 (proposed) along Tana River (Source: Survey of Kenya, Sheet 124)

Diversion site 2 (Proposed)

Diversion site 3 (proposed)

APPENDIX D3: Flood prone areas and potential road blocks of Kenya (Source: United Nations office for the Coordination of Humanitarian Affairs (OCHA), 2009)

FLOOD PRONE AREAS AND POTENTIAL ROAD BLOCKS